

1 Dear editor and reviewer,
2 Thank you for your positive comments and very important recommendations to improve our
3 manuscript. We have carefully modified the manuscript based on your suggestions and provide a
4 response to each comment. The paper have been polished by a native English speaker. The following
5 revise are based on two reviewers suggestions. Reviewer comments are given in black, and
6 responses are given in blue. Below we provide a marked-up manuscript version showing the changes
7 based on your comments. The main modifications to the manuscript are as follows:

- 8 1. Fig. 10 and Table 7 were revised according to the reviewers suggestions.
- 9 2. We revised the description in Abstract, Section 4.2 and, Section 5 accordingly.
- 10 3. We change the term of “Total SWE” to “snow mass” in whole manuscript

11

12 Please see below the detailed responses (in blue color).

13

14 **REVIEWER 1#**

15 In this manuscript, the authors use a support vector regression (SVR) algorithm that they
16 developed in a previous paper to estimate snow depth from passive microwave observations.

17 In addition to evaluating their estimates of snow depth against values from GlobSnow and
18 ERA-Interim/Land, they also use snow density assumptions to estimate snow water equivalent
19 (SWE) for the Northern Hemisphere. Their major conclusion is that SWE has been declining
20 by $\sim 5\ 800\ \text{km}^3$ a year, or approximately $139\ 200\ \text{km}^3$ over their 24-year study period. The
21 authors say this decline is equivalent to a 12.5% reduction of SWE over the study period,
22 suggesting the initial amount of SWE was $1113\ 600\ \text{km}^3$.

23 I believe there is a fundamental flaw in how the authors are calculating annual snow
24 accumulation in this manuscript. Their estimate of annual SWE is orders of magni- tude larger
25 than other global datasets suggest. Mudryk et al. (2015) show that the Northern Hemisphere has an
26 average annual snow accumulation of $3500\ \text{km}^3$ (see Figure 1a, taken from Figure 3 in that
27 manuscript). Using four commonly used global datasets (ERA-Interim, GLDAS, MERRA2, and
28 VIC), I estimate the long-term-average global snow storage to be $\sim 4000\ \text{km}^3$ (see Figure 1b). Even
29 if these global models/reanalyses are underestimating SWE, it is unlikely they are wrong by as much
30 as this manuscript indicates. I believe the authors may be summing daily values of SWE when
31 calculating their annual total SWE, as one would do when calculating annual precipitation from
32 daily precipitation values. However, this is incorrect when working with SWE. Instead, the authors
33 should consider comparing the annual maximum SWE over their period of record. This will not lead
34 to such a dramatic value of SWE decline, but I think it would be interesting to see how their method
35 compares to changes in SWE from GlobSnow, ERA-Interim/Land, and other global data products.

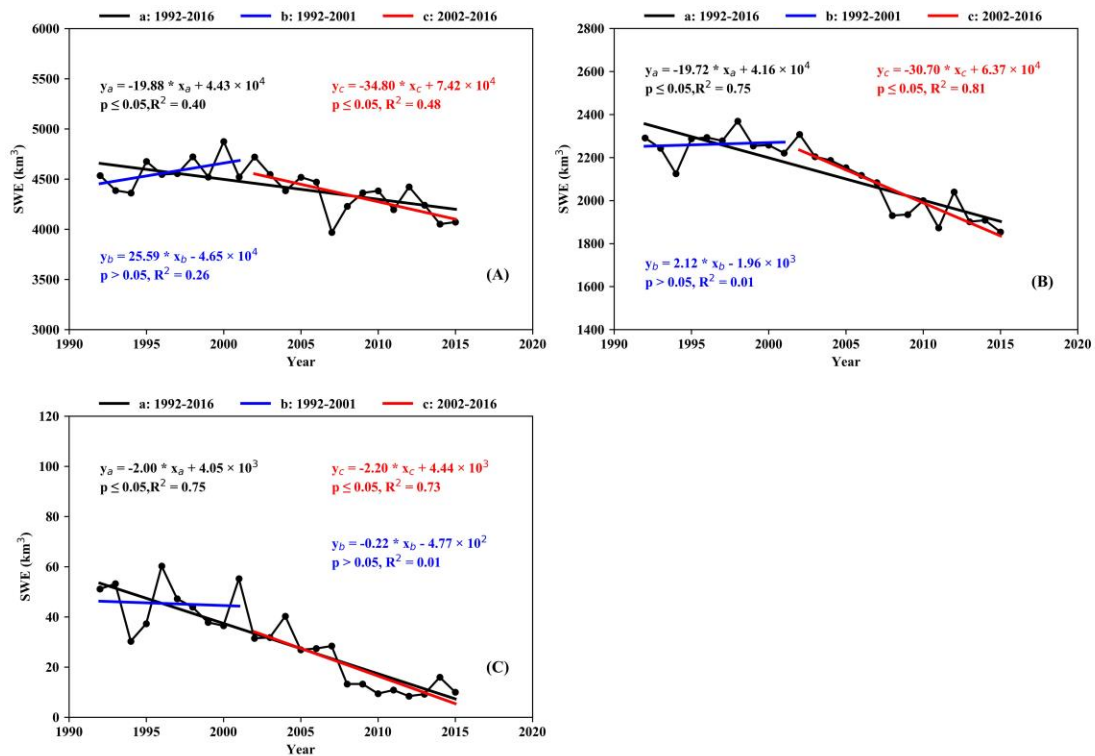
36 With this mistake, the manuscript is not ready for publication. But if the authors redo their SWE
37 calculations and the following analyses, I would be interested to see the SWE results from their
38 SVR method. Since this error is critical to the main conclusions of the manuscript, I do not include
39 a review of the rest of the paper.

40 Reference: Mudryk, L. R., Derksen, C., Kushner, P. J., and Brown, R.: Characterization of Northern
41 Hemisphere Snow Water Equivalent Datasets, 1981–2010, *Journal of Climate*, 28, 8037-8051.

1
2
3
4
5
6
7
8
9

Response: Thank you very much for your review of our manuscript. We appreciate your positive comments and very useful suggestions for improving the manuscript. We made modification according to your suggestion.

1. The analysis indexes were changed. In Fig. 10, we used annual maximum snow mass, annual average snow mass and annual minimum snow mass to analyze the variation characteristic of snow mass over the past 25 years (1992-2016). The average annual maximum snow mass of NHSnow SWE products have quite same magnitude as the analysis datasets provides by the reviewers and Mudryk et al. (2015).



10
11
12
13
14
15
16
17
18
19
20
21
22
23
24
25
26

Figure 10. Interannual variation of annual maximum snow mass (A), annual average snow mass (B) and annual minimum snow mass (C) over the Northern Hemisphere for three period 1992-2016 (black line), 1992-2001 (blue line), and 2002-2016 (red line). Trends estimates were computed from least squares. P is the confidence level for the coefficient estimates; R2 is the goodness of fit coefficient.

Subsequently, we mainly revised the description of Paragraph 2 in Section 4.2, the updated description as flowing (from page 16 lines 18 to page 17 line 13):

“

The snow mass variation characteristic over the past 25 years were explored by interannual variation (Fig. 10) and intra-annual cycles (not show figure) of snow mass over the Northern Hemisphere . Figure 10 depicts the time series of interannual variation of annual maximum, average and minimum snow mass with respect to 1992–2016 period. The biggest value of annual maximum snow mass occurred in 1998–1999 up to 4875 km3, while the least was 3969 km3 in 2007-2008. The annual maximum snow mass present particularly significant decreasing trends ($P \leq 0.05$) during 1992 – 2016, at the rate of approximately -19.88 km3 yr.-1 (Fig. 10A). Trend analysis reveals that annual

1 maximum snow mass have a 8% reduction from 1992 to 2016. Note that it present a increase
 2 variation trend by about 25.59 km³ yr.⁻¹ ($P > 0.05$) rate for 1992-2001. In contrast, the annual
 3 maximum snow mass exhibits a significantly decrease trends (with -34.80 km³ yr.⁻¹, $P \leq 0.05$)
 4 since 2002, which would lead to a extraordinary decrease during 1992 – 2016. According to the
 5 static, the annual maximum snow mass usually appear in February (about 60%) and March (about
 6 40%), and in recent several years this occurred in March become a normal state. This finding needs
 7 to be further analyzed in the future work by correlation with climatic factors, such as precipitation
 8 effects (Kumar et al., 2012). We find that the biggest and the least value of annual average snow
 9 mass respectively appear in 1998-1999 (~2370 km³) and 2015-2016 (~1850 km³) in Fig 10B.
 10 Likewise, in Fig 10B and 10C the annual average (minimum) snow mass exhibit a significant
 11 decrease trend in 1992-2016 period by rate -19.72 km³ yr.⁻¹, $P > 0.05$ (-2.00 km³ yr.⁻¹, $P \leq 0.05$)
 12 and 2002-2016 period at a rate of -30.70 km³ yr.⁻¹, $P > 0.05$ (-2.2 km³ yr.⁻¹, $P \leq 0.05$). For 1992-
 13 2016 period, the variation tendency of annual average (minimum) snow mass do not pass the
 14 significance level test. Moreover, the reduction for the annual average and annual minimum snow
 15 mass is 13% and 67%, respectively.”

16
 17 2. We changed the original snow mass calculation method. The revised Table 7 show the variation
 18 of monthly average snow mass.

19 Table 7. Variation rate and changes of monthly average snow mass during 1992-2016. The asterisk
 20 indicate that the changes are significant at 95% confidence level. The changes was calculated with
 21 respect to the average of monthly average snow mass on 25 years.

Month	Variation rate (km ³ /yr.)	% The percentage of Changes
September	-5.96*	-63.89%
October	-25.50*	-43.99%
November	-36.50*	-26.96%
December	-32.66*	-5.00%
January	-34.38*	-9.53%
February	-30.89*	-11.91%
March	1.90	-4.30%
April	-4.29	-6.46%
May	-11.33*	-19.59%
June	-8.01*	-64.67%

22
 23
 24 We revised the description of Paragraph 3 (from page 17 line 18 to page 18 line3) to flowing
 25 statement:

26 “
 27 When analyzing long-term variation of monthly average snow mass (refer to Eq. B in Appendix),
 28 ten months (September to June) exhibit significant decreasing apart from March and April (Table
 29 7). The maximum decrease rate was approximately -36.50 km³ yr.⁻¹ ($P \leq 0.05$) in November
 30 while the minimum decrease occurred in April at -4.29 km³ yr.⁻¹ ($P > 0.05$). However, there are no
 31 significant trends in March and April with large interannual variations (Table 7). Compared with the
 32 fall (September to November) and spring (March to June), the interannual variability of monthly
 33 average snow mass significantly decreased in winter (December to February), with average rate of

1 less than $-32 \text{ km}^3 \text{ yr}^{-1}$. The reduction of monthly average snow mass in ten month were generated
2 using the average pattern of each month over 1992-2016 as a reference. We found that the reduction
3 of monthly average snow mass fluctuated ranging from -65% to -4% for each month (September to
4 June) over 1992-2016 (Table 7). The largest and smallest reduction were about 64.67% and 4.30% ,
5 which occurred in June and March, respectively. Variation analysis of monthly average snow mass
6 could offer a powerful evidence for annual average snow mass exhibit a significantly decreasing
7 tendency (Table 7, Fig. 10B).

8 ”

9
10 3. We changed “Similar conclusions also appear in total SWE change analysis. The total SWE shows
11 a 12.5% reduction and the monthly average total SWE is 65.8% for the largest reduction and a 4.2%
12 for least reduction which occur in June and March, respectively. The total SWE report well-
13 documented significant decreasing trends ($P < 0.05$) during the study period.” to “Similar
14 conclusions also appear in snow mass change analysis. The annual maximum, average and minimum
15 snow mass exhibit significantly decrease trends and respectively show a 8% , 13% and 67%
16 reduction. The monthly average snow mass has shown a decreasing trend almost in every month
17 and the reduction range from 64.67% (June) to 4.3% (March). The annual average snow mass report
18 well-documented significant decreasing trends ($\sim 20 \text{ km}^3 \text{ yr}^{-1}$, $P < 0.05$) during the study period.”
19 in page 21 lines 10-16.

20
21 4. In Abstract “Further analysis were performed across the Northern Hemisphere during 1992-2016,
22 which used snow depth, total snow water equivalent (snow mass) and, snow cover days as indexes.
23 Analysis showed the total snow water equivalent has a significant declining trends ($\sim 5794 \text{ km}^3 \text{ yr}^{-1}$,
24 12.5% reduction)” were revised to “Further analysis were conducted across the Northern
25 Hemisphere during 1992-2016 using snow depth, snow mass and, snow cover days as indexes.
26 Results showed that annual average snow mass had a significant declining trend with a rate of about
27 $19.72 \text{ km}^3 \text{ yr}^{-1}$ or 13% reduction in snow mass” in page 1 lines 21-25.

28
29

Spatiotemporal variation of snow depth in the Northern Hemisphere from 1992 to 2016

Xiongxin Xiao^{1,2}, Tingjun Zhang^{1,4}, Xinyue Zhong³, Xiaodong Li¹, Yuxing Li¹

¹Key Laboratory of Western China's Environmental Systems (Ministry of Education), College of Earth and Environment Sciences, Lanzhou University, Lanzhou 730000, China

²School of Remote Sensing and Information Engineering, Wuhan University, Wuhan 430079, China

³Key Laboratory of Remote Sensing of Gansu Province, Cold and Arid Regions Environmental and Engineering Research Institute, Chinese Academy of Sciences, Lanzhou 730000, China

⁴University Corporation for Polar Research, Beijing 100875, China.

Correspondence to: Tingjun Zhang (tjzhang@lzu.edu.cn)

Abstract: Snow cover is an effective ~~best~~ indicator of climate change due to its ~~effect~~ impact on regional and global surface energy and, water balance, thus weather and climate, hydrology hydrological process and water resources, ~~climate~~, and ecosystem as a whole function. The overall objective of this study is to investigate changes and variations of snow depth and snow mass over the Northern Hemisphere from 1992 to 2016. We developed a long term Northern Hemisphere daily snow depth and snow water equivalent product (NHSnow) by ~~the applying~~ application of the support vector regression (SVR) snow depth retrieval algorithm ~~to historical~~ using passive microwave ~~sensors~~ remote sensing data from 1992 to 2016. ~~The accuracies of the s~~ Snow depth products were evaluated against observed snow depth at meteorological stations along with the other two snow cover products (GlobSnow and ERA-Interim/Land) across the Northern Hemisphere. The evaluation results showed that NHSnow performs generally well with relatively high accuracy (bias: 0.59 cm, MAE: 15.12 cm and RMSE: 20.11 cm). Further analysis were ~~performed~~ conducted across the Northern Hemisphere during 1992-2016, ~~which used~~ using snow depth, snow mass and, snow cover days as indexes. ~~Analysis-Results~~ showed that annual average the snow mass has had a significant declining trends with a rate of about 19.72 km³ yr.⁻¹ or 13% reduction in snow mass (-5794 km³ yr.⁻¹, 12.5% reduction). Although spatial variation pattern of snow depth and snow cover days exhibited slight regional differences, it generally reveals a decreasing trend over most of the Northern Hemisphere. Our work provides evidence that rapid changes in snow depth and snow ~~water equivalent~~ mass are occurring since the beginning ~~at the turn~~ of the 21st century accompanied with dramatic climate, ~~surface based~~ warming.

1 1. Introduction

2 Seasonal snow cover is an important component of the climate system and global water cycle that
3 stores large amounts of freshwater and have significant~~play major~~ impacts on the surface energy and
4 water budget, thus weather and climate, hydrological processes and water resources, heat and mass
5 exchange between the ground surface and the atmosphere, and ecosystem as a whole~~climatology and~~
6 ~~water management~~ (Immerzeel et al., 2010;Zhang, 2005;Robinson and Frei, 2000;Tedesco et al., 2014).

7 On account of the high albedo and low heat conductivity properties of snow, snow cover may directly
8 modulate the land surface energy balance (Flanner et al., 2011), influence on soil thermal regime
9 (Zhang et al., 1996;Zhang, 2005), and indirectly affect atmospheric circulation (Cohen et al.,
10 2012;Zhang et al., 2004;Li et al., 2018). Most jurisdictions in the Northern Hemisphere rely on natural
11 water storage provided by snowpack (Diffenbaugh et al., 2013;Barnett et al., 2005), supplying water for
12 domestic and industrial usage (Sturm, 2015;Qin et al., 2006). Accurate estimation of and reliable
13 information on snow cover spatial and temporal change at regional and global scales is very critical for
14 climate change monitoring, model evaluation and water resources management (Brown and Frei,
15 2007;Flanner et al., 2011).

16 Snow depth (SD) is the most useful and commonly measured parameter at national metrological
17 and hydrological stations, numerous research sites, and sites for local and regional water resources
18 assessment programs~~using in situ observations~~. Given the sparseness of measurements, it is not possible
19 to fully capture spatial variability of snow cover, especially at high altitude mountains and high latitude
20 regions. Although ~~the in-situ observations~~ method is can obtain accurate and relative reliable SD and
21 snow water equivalent (SWE) data, it is unrealistic in mountain regions and low population zones because
22 it is labor intensive and high costs, ~~material and financial resource intensive~~. Remote sensing is the most
23 effective and powerful way of obtaining information of snow cover over larger areas (Foster et al., 2011).
24 Optical remote sensing is capable of observing large areas of snow cover; however, it is unable to observe
25 the Earth's surface under cloudy conditions (Foster et al., 2011;Che et al., 2016;Dai et al., 2017).
26 However, microwave remote sensing has this potential and is an attractive alternative to optical remote
27 sensing under all weather conditions and round the clock. It can also be used to estimate SD and ~~snow~~
28 ~~water equivalent (SWE)~~ due to the interaction with snowpack by providing dual polarization data at
29 different frequencies (Chang et al., 1987;Che et al., 2008;Takala et al., 2011).

1 Snow cover products derived from [\(PM\)](#) passive microwave ~~(PM)~~ data have been widely applied to
2 investigate regional and global climate change, and validate hydrological and climate models (Brown et
3 al., 2010;Brown and Robinson, 2011;Dai et al., 2017). Progress in satellite data acquisition, as well as
4 SD/SWE retrieval algorithm development, have led to a global improvement in snow monitoring (Qin et
5 al., 2006;Snauffer et al., 2016). The PM brightness temperature of the SMMR (Scanning Multichannel
6 Microwave Radiometer), SSM/I (Special Sensor Microwave Imager), AMSR-E (Advanced Microwave
7 Scanning Radiometer for Earth Observing System), AMSR2 (Advanced Microwave Scanning
8 Radiometer 2 on the Global Change Observation Mission – Water), SSM/I~~S~~ (Special Sensor Microwave
9 Imager), SSM/I~~I~~ (Special Sensor Microwave Imager Sounder) and, FY-3B/C (Fengyun-3 satellite B/C)
10 are available and several algorithms have been developed to estimate SD and SWE ~~using PM brightness~~
11 ~~temperature data~~ (Chang et al., 1987;Dai et al., 2012;Xiao et al., 2018;Pulliainen, 2006;Takala et al.,
12 2011;Che et al., 2008;Foster et al., 1997).

13 Most retrieval algorithms operate on the principle that the difference in brightness temperature
14 between 18 and 37 GHz reflects the quantity of SD and SWE (Chang et al., 1987). Over and
15 underestimated trends are prevalent in these linear SD and SWE retrieval algorithms (Gan et al., 2013)
16 for which there are two possible and reasonable explanations. One is that vegetation overlaying snow
17 attenuates its microwave scatter signal and results in underestimating SD and SWE from PM data (Che
18 et al., 2016;Vander Jagt et al., 2013). To reduce the effect of tree canopy, a forest fraction was introduced
19 into retrieval algorithm developed to estimate SD and SWE (Foster et al., 1997;Che et al., 2008), or the
20 retrieval algorithm was constructed based on particular land cover types (Goïta et al., 2003;Che et al.,
21 2016;Derksen et al., 2005;Foster et al., 2009). The other explanation is that the relationship between
22 snow properties (SD or SWE) and the PM brightness temperature is non-linear. Newer approaches (e.g.
23 artificial neural networks, support vector regression, decision tree) have emerged using data-mining and
24 have been explored to retrieve SD and SWE that are intended to replace traditional linear methods
25 (Gharaei-Manesh et al., 2016;Tedesco et al., 2004;Liang et al., 2015;Forman et al., 2013;Xue and Forman,
26 2015). However, there ~~are~~ remain some limitations for these retrieval algorithms due to the diversity of
27 land cover types and the spatiotemporal heterogeneity of snow physical properties.

28 Numerous studies have reported the changes in snow cover extent (SCE) at regional and
29 hemispheric scales (Rupp et al., 2013;Dai et al., 2017;Derksen and Brown, 2012;Brown and Robinson,
30 2011;Huang et al., 2016). Huang et al. (2017) reported the impact of climate and elevation on snow cover

1 variation in Tibetan Plateau, including SWE, ~~snow cover area~~[SCE](#) and, snow cover days. Hori et al.
2 (2017) developed a 38-year Northern Hemisphere daily ~~snow cover extent~~[SCE](#) product and analyzed
3 seasonal Northern Hemisphere ~~snow cover extent~~[SCE](#) variation trends. In this study, SD was selected
4 as basis for analyzing spatiotemporal change of snow cover. SD provides an additional dimension to
5 snow cover characteristics. Barrett et al. (2015) explored intra-seasonal variability in springtime Northern
6 Hemisphere daily SD change by the phase of the Madden–Julian oscillation. Wegmann et al. (2017)
7 compared four long-term reanalysis datasets with Russian SD observation data. However, this study only
8 focused on snowfall season (October and November) and snowmelt season (April). SD change trends
9 have also been analyzed at regional scales (Ye et al., 1998;Dyer and Mote, 2006). Several studies
10 quantified the spatial and temporal changes consistency of SWE or snow mass derived from satellite data
11 [and reanalysis data](#) (Mudryk et al., 2015) but these studies have focused on the limited dimension of
12 snow cover variation. Dyer and Mote (2006) used a gridded dataset to study regional and temporal
13 variability of SD trends across North America from 1960-2000 (~~Dyer and Mote, 2006~~) and [Foster et al.](#)
14 (2009).[reported](#) the characteristic of seasonal ~~snow extent~~[SCE](#) and snow mass in South America ~~ferom~~
15 1979 to 2006 was described. ~~and reported~~

16 There are, however, very limited data (station data, satellite data or otherwise) that can provide both
17 SD and SWE on a hemispheric scale. This [paper study](#) describes ~~the an~~ approach to develop a consistent
18 25-year of daily SD and SWE of Northern Hemisphere utilized multi-source data. The primary objective
19 of this study is to develop 25 years (1992-2016) hemispherical SD and SWE products (hereafter referred
20 to as the NHSnow) with a 25 km spatial resolution using [support vector regression](#) (SVR) SD retrieval
21 algorithm (Xiao et al., 2018). This paper will address the following questions: 1) How consistent are
22 NHSnow and other sourced snow cover datasets with ~~the in in~~-situ SD observations? 2) What is the
23 spatiotemporal variability of [SD and snow mass](#)~~snow cover~~ in the Northern Hemisphere from 1992-2016?
24 Meanwhile, it is extremely challenging to make extensive quantitative validation of SD and SWE
25 estimates.

26 This paper is organized in [the following](#) five sections, ~~as follows~~. [After the introduction section with](#)
27 [literature review, the S](#)ection 2 describes the data sets used in this study. The methods of data
28 preprocessing and snow cover products generation ~~were are~~ provided in Section 3. Next, we describe
29 NHSnow validation against in-situ snow observation ~~records~~, ~~exhibit~~ [demonstrate](#) the variability of
30 snow cover in the Northern Hemisphere and discuss the potential ~~effect~~ [controlling](#) factors for the

1 variations ~~of snow cover results~~ utilized NHSnow data (Section 4). Finally, section 5 summarizes the
2 work of this paper.

3 **2 Datasets**

4 **2.1 Passive microwave data**

5 ~~Because~~ Cloud often appears in the snow cover regions ~~or condition~~, ~~during and~~ the winter season
6 often conceals snowfall possibility ~~which make~~, ~~here is~~ particularly advantageous ~~for~~ using passive
7 microwave remote sensing ~~to detect SCE and SD~~. The SSM/I and SSMIS is PM radiometer onboard ~~the~~
8 United States Defense Meteorological Satellites Program (DMSP) satellite (~~data~~ available from the
9 National Snow and Ice Data Center, <http://nsidc.org/data/NSIDC-0032>). The SSM/I (F11 and F13)
10 dataset from this platform, as well as SSMIS (F17), present with the equal-area scale earth grid (EASE-
11 Grid) format and 25 km spatial resolution (Brodzik and Knowles, 2002; Armstrong, 2008; Wentz,
12 2013; Armstrong and Brodzik, 1995) (Table 1). The ~~snow cover area~~ ~~SCE~~ and SD derived from SSM/I
13 (F11) and SSM/I (F13) data have high consistency rendering the calibration between these two sensors
14 for snow cover area and SD unnecessary (Dai et al., 2015). To minimize the melt-water effect to some
15 extent, which can change the microwave emissivity of snow, only descending orbit (nighttime) passive
16 microwave data were used (Foster et al., 2009).

17 **2.2 Ground-based data**

18 ~~Daily ground based~~ SD ~~measurements~~ ~~observation~~ are used to construct and verify the SD retrieval
19 model in this study from two sources ~~of daily SD observation~~. The first ~~dataset~~ is the Global Surface
20 Summary of the Day (GSOD) dataset provided by National Oceanic and Atmospheric Administration
21 (NOAA) (<https://data.noaa.gov/dataset/dataset/global-surface-summary-of-the-day-gsod>). This online
22 dataset, which began in 1929, is derived from the Integrated Surface Hourly (ISH) dataset (Xu et al.,
23 2016). There are fourteen daily elements in GSOD dataset, including SD measured at 0.1 inch. The
24 missing ~~of~~ SD ~~measurement~~ or reported 0 on the day would be marked 999.9. Data at approximately
25 30000 meteorological stations were recorded of which ~~more than~~ 9000 ~~typically~~ are ~~typically~~
26 ~~obtainable~~ ~~valid~~. In our study period and area, more than 17 000 meteorological station were selected
27 with records from 1991 ~~to 2016~~. ~~All meteorological sites and stations are~~ ~~and a location~~ far ~~away~~ from
28 large water bodies ~~such as large rivers, lakes, and oceans~~.

1 To supplement data from stations that were not reporting during the ~~study~~[1991 to 2016](#) periods,
2 ground-based measurements of daily SD were gathered from an additional 635 Chinese meteorological
3 stations available at the National Meteorological Information of China Meteorological Administration
4 (Xiao et al., 2018;Zhong, 2014). These daily SD records begun in 1957 include SD (unit, cm),
5 observation time, and geographical location information available (<http://data.cma.cn/en>).

6 **2.3 Topographic and land cover data**

7 We also used topography as an auxiliary information to estimate SD (Xiao et al., 2018). Elevation
8 was available from ETOPO1 at a resolution of 1 arc-minute (Amante, 2009) available at
9 (<http://www.ngdc.noaa.gov/mgg/global/>). To match the resolution of the PM brightness temperature data
10 with 25 km spatial resolution, we resampled the ETOPO1 to 25 km resolution (Fig. 1).

11 To increase the accuracy of SD estimates for different land cover types, we ~~both~~-used [both the](#)
12 MODIS land cover (MCD12Q1 V051) from 2001 to 2013 (Friedl and Sulla-Menashe, 2011;Friedl et al.,
13 2010) and [the](#) Advanced Very High Resolution Radiometer (AVHRR) Global Land Cover classification
14 generated by the University of Maryland Department of Geography. The MCD12Q1 International
15 Geosphere-Biosphere Program (IGBP) classification scheme divides land surface into 17 types, which
16 were reclassified into five classes according to Xiao et al (2018) study.

17 AVHRR imagery was acquired between 1981-1994 from the NOAA-15 satellite (Hansen et al., 2000)
18 and were categorized into fourteen land cover classes at 1 km resolution. These data allowed us to adjust
19 the proposed snow-depth retrieval algorithm by reclassifying the fourteen native land cover classes into
20 five classes (water, forest, shrub, prairie and, bare-land) at 25 km spatial resolution (Table A.). MCD12Q1
21 is available at site <https://earthdata.nasa.gov/>, while AVHRR land cover data is available from
22 <http://www.landcover.org/data/landcover/>.

23 **2.4 Satellite snow cover datasets**

24 Two kinds of snow cover datasets were utilized based on two criteria: covering the Northern
25 Hemisphere and long-term availability. We selected GlobSnow and ERA-Interim/Land which are widely
26 used in global and regional climate change studies (Snauffer et al., 2016;Hancock et al., 2013;Mudryk et
27 al., 2015). These datasets were used to compare with the NHSnow SD product.

28 In November 2013, the European Space Agency (ESA) released the GlobSnow Version 2.0 SWE

1 and Snow Extent (SE) data for the Northern Hemisphere (Takala et al., 2011; Pulliainen, 2006). These
2 data include all non-mountainous areas in the Northern Hemisphere and are available online
3 (<http://www.globsnow.info/>). Processing includes data assimilation based on combining satellite PM
4 remote sensing data (SMMR, SSM/I and SSMIS), spanning December 1979 to May 2016, with ground-
5 based observation data in a data assimilation scheme to derive SWE. GlobSnow Version 2.0 (hereinafter
6 referred as GlobSnow) provides three kinds of temporal aggregation level products with 25 km spatial
7 resolution: daily, weekly and monthly. This dataset covers all land surface areas in a band between 35°
8 N ~ 85° N excluding mountainous regions, glaciers and Greenland. To convert between SD and SWE
9 using GlobSnow, the snow density is held constant at 0.24 g/cm³ [which is from](#) (Sturm et al.,
10 2010; Hancock et al., 2013; Che et al., 2016).

11 ERA-Interim/Land (Balsamo et al., 2015) is a global land-surface reanalysis product with data from
12 January 1979 to December 2010 based on ERA-Interim meteorological forcing. It is produced by a land-
13 surface model simulation using the Hydrology Tiled ECMWF Scheme of Surface Exchange over Land
14 (HTESSEL), with meteorological forcing from ERA-Interim. Dutra et al. (2010) described the snow
15 scheme and demonstrated the verification using field experiments. [SWE, which is labeled as SD in this](#)
16 [dataset](#) “SD”, ~~which actually is SWE~~, is one of the thirteen parameters provided. We ~~should~~ [converted](#)
17 SWE to SD using the associated snow density data. These two datasets are available online
18 (<http://apps.ecmwf.int/datasets/data/interim-land/type=an/>). To ~~maximize~~ the proximity to the
19 descending orbit time of passive microwave sensor, the data with analysis type at 6 o'clock were used in
20 this study, and the spatial resolution of these data is 0.125 degree.

21 **2.5 Snow classification data**

22 In order to accurately estimate SWE, snow classification data were used to convert SD into SWE.
23 Global Seasonal Snow Classification System was defined by Sturm et al. (1995) based on snow physical
24 properties (SD, thermal conductivity, snow density snow layers, degree of wetting, etc.), and seasonal
25 snow cover. Snow cover ~~were~~ [was](#) categorized into six snow classes (tundra, taiga, alpine, maritime,
26 prairie, and ephemeral) plus water and ice fields (Figure 2). Snow classification data can be accessed
27 from the National Center for Atmospheric Research (NCAR)/Earth Observing Laboratory (EOL)
28 (<https://data.eol.ucar.edu/dataset/6808>). The snow classification dataset was developed and tested for the
29 Northern Hemisphere at 0.5-degree spatial resolution (Sturm et al., 1995).

1 3 Methods

2 3.1 Theoretical basis

3 Snow distribution is affected by various factors, but not limited to, vegetation (Che et al.,
4 2016;Vander Jagt et al., 2013), soil and air temperature (Forman and Reichle, 2015;Grippa et al.,
5 2004;Dai et al., 2017), topography and wind (Smith and Bookhagen, 2016). [The snow retrieval process](#)
6 [uses various parameters](#)~~The snow retrieval process uses DS and other parameters (A, T, G, L, D ...)~~ to
7 yield snow parameters (e.g. SD, Eq. 1) (Xiao et al., 2018).

$$[S] = g(A, T, G, L, DS, D \dots) + \varepsilon \quad (1)$$

8 where $g(\cdot)$ denotes the retrieval function. DS is the digital signal from remote sensing sensor (PM, active
9 microwave, visible spectral remote sensing etc.), A is the atmosphere (wind speed, air temperature,
10 humidity, precipitation etc.), T is the topography (latitude, longitude, elevation, terrain slope, aspect etc.),
11 L is the location (latitude, longitude), G is the ground (ground surface temperature, vegetation type etc.),
12 S is the snow properties (snow grain size, density, reflectance, SD, SWE etc.), D is the day of year and ε
13 is the residual error or uncertainty that describes the relationship between sensor signal and measured
14 snow properties.

15 The SVR SD retrieval algorithm also follows the snow retrieval process (Eq. 1). We utilized ten
16 parameters were as input parameters, including PM brightness temperature (19 GHz, 37 GHz, 85 GHz,
17 or 91 GHz) with vertical and horizontal polarizations, geophysical location (latitude and longitude),
18 elevation and, the measured SD. The output parameter is the estimated SD. Apart from above factors, the
19 SVR SD retrieval algorithm also considers other influence factors, including wet snow, land cover types
20 and day of year (Xiao et al., 2018) to improve the accuracy of estimated SD. Day of year have been
21 converted into three snow cover stages, which mean indirectly considering snow properties evolution.

22 3.2 Processing flow overview

23 The SVR SD retrieval algorithm ~~first proposed~~[developed](#) by Xiao et al. (2018), which indirectly
24 considers seasonal variation and vegetation influence in the evolution of snow properties, was used to
25 estimate SD. In Eurasia, it was found that the SVR SD retrieval algorithm performs much superior with
26 reduced uncertainties compared based upon the correlation coefficient (R), mean absolute error (MAE),
27 and root mean squared error in Xiao et al. (2018) study. It should be noted that this study used daily

1 observation in the Northern Hemisphere with exception of July and August. ~~Here, we provide more~~
2 ~~detailed but different descriptions for the SVR SD retrieval algorithm in several steps (Fig. 3).~~ We shortly
3 describe the SVR SD retrieval algorithm involved six steps (see Fig. 3): step 1 is preprocessing
4 meteorological station SD measurement data and PM brightness temperature data; Before estimating SD
5 using PM data, it is necessary to identify snow cover and dry snow by a set of criteria in step 2; To
6 segregate the land cover effect on snow cover distribution (step 3) and snow properties evolution effect
7 (step 4), SD retrieval model were established on different land cover types (forest, shrub, prairie, bare-
8 land) and snow cover stages (snow cover accumulation, stabilization and ablation stage); in step 5, we
9 chose SVR as retrieval function (Eq. 1) with specific kernel functions and parameters; step 6 is
10 constructing a set of SD retrieval models trained by the suitable size and quality training samples. The
11 more detailed descriptions of these ~~other~~ steps can refer to the Xiao et al ~~paper~~ (2018) ~~not repeated here~~.
12 ~~Here, we provide more detailed but different descriptions for the SVR SD retrieval algorithm in several~~
13 ~~steps (Fig. 3)~~

14 Step 3. Due to the our study period pre-dates MODIS data, we used AVHRR land cover as
15 supplement data. MODIS and AVHRR land cover were reclassified into four classes (forest, prairie, shrub
16 and bare-land) which were bases of constructing SD retrieval sub-model. Table A (in appendix) describes
17 the reclassification scheme of AVHRR land cover ~~is described~~. MODIS land cover reclassification
18 schemes were documented in Xiao et al. (2018). Because of the relative stability of land cover change,
19 MODIS land cover in 2013 was used for each year during 2013–2016. Similarly, MODIS land cover in
20 2001 was used in each year during 1998–2001, and AVHRR land cover data were used ~~for 6 years from~~
21 ~~(1992 through–1997).~~

22 Step 6.1 Construction of a subcontinental model. It needs to be stressed that the snow properties in
23 the Eurasia (~~EU~~) and North America (~~NA~~) exhibit noticed discrepancy especially in snow density. (Zhong
24 et al., 2014; Bilello, 1984). One study pointed out that mean snow density in the former Soviet Union
25 (0.21 ~ 0.31 g/cm³) was lower than the data from ~~NA~~ North America (0.24 ~ 0.31 g/cm³) (Bilello, 1984),
26 and also Zhong et al. (2014) explained the possible reasons which resulting in the diversity of snow
27 density in ~~EU~~ Eurasia and ~~NA~~ North America. Based on this, we separately constructed the SD retrieval
28 models for ~~EU~~ Eurasia and ~~NA~~ North America.

29 Step 6.2 Training dataset selection is the process of removing redundant features from spatial data.
30 The accuracy of estimated SD primarily depends on training data quality, which also demonstrate the

1 significance of the selection rule of training samples (Xiao et al., 2018). Inputting more data than needed
2 in the training dataset to train SD retrieval model, may lead to overfitting and an estimated SD with high
3 error. In this study, we collected an extremely large number of daily SD records over 25 years,
4 necessitating a optimized selection rule to avoid data information redundancy.

5 The selection rule proposed in previous research (Xiao et al., 2018) was modified and then it was
6 divided into two steps ~~in~~ here. Firstly, the numbers of sample in the three layers [that split up by snow](#)
7 [depth should be concretely quantified, i.e.](#); layer1 ($0 \leq SD < 50$; [low snow](#)), layer2 ($50 \leq SD < 100$; [medium](#)
8 [depth](#)) and layer3 ($SD \geq 100$; [high depth](#)), should be concretely quantified. To avoid an inflated training
9 sample in layer2 and layer3, we set a threshold (3 000) determined by several tests (not shown). A
10 threshold (12000) for layer1 was adopted following Xiao et al. (2018). Table 2 [summarizes](#) the section
11 of training sample for each layer in detail. After that, the quality of training sample in each layers
12 determined by stratified random sampling is the second step. Stratification was performed in 1 cm SD
13 intervals. Note that, all ~~the selected on~~ operations ~~in~~ here were randomly performed.

14 Step 7. Through above steps, the daily estimated SD data in the Northern Hemisphere from January
15 1992 to December 2016 (excluding July and August) were obtained. Owing to the nature of radiometer
16 observations, NHSnow products are only reliable in areas with seasonal dry snow cover. Areas with
17 sporadic wet or thin snow are not reliably detected and areas marked as snow-free may include areas
18 with wet snow. If one pixel is detected as snow cover by the detection decision tree (Grody and Basist,
19 1996), but is likely to be shallow ~~or medium to deep~~ snow with an estimated value of equal or less than
20 1 cm, the SD value is set as 5 cm (Che et al., 2016; Wang et al., 2008) (Fig. 4.).

21 Step 8. In this study, Greenland and Iceland are excluded from the generation and analysis of
22 NHSnow (NH_SD, NH_SWE) products due to their complex coastal topography and the difficulty in
23 discriminating snow from ice (Fig. 4) (Brown et al., 2010). Missing data and zero-data gaps occur in the
24 process of generating daily SD gridded products. Therefore, the following filters were applied. Daily
25 estimated SD was averaged with a sliding 7-day window to reduce noise and compensate for missing
26 data in the daily time series. For example, the SD estimate for 4 January is an average of the assimilated
27 scheme output for 1 to 7 January (Takala et al., 2011; Che et al., 2016). When finished, the sliding SD
28 method generated daily SD products for the entire Northern Hemisphere (NH_SD; Fig. 4).

1 3.3 Estimation of SWE

2 SWE contains more useful information for hydrologists than SD because it represents the amount
3 of liquid water in the snowpack [useful for studies on surface hydrological processes and for assessing](#)
4 [water resources when available to the ecosystem as the](#) snow melts. One way to estimate SWE [is to use](#)s
5 SD and snow density (ρ_{snow}) as described in Eq. 2. Northern Hemisphere SWE products were generated
6 in this study using snow density that converts SD to SWE. (Eq. 2, Fig. 3 and 4, Step 9).

$$SWE(mm) = SD(cm) \times \rho_{snow}(g/cm^3) / \rho_{water}(g/cm^3) \times 10 \quad (2)$$

7 At present, the primary problem is to obtain relatively accurate snow density. In this study,
8 dynamical calculation methods were adopted to estimate snow density. Two methods are usually used to
9 convert SD to SWE. The first [method](#) uses a fixed value, 0.24 g/cm³ (or other value), without
10 spatiotemporal variation (Che et al., 2016; Takala et al., 2011). The second uses a temporally static by
11 spatially variable mask of snow density to estimate SWE and are used to generate current AMSR-E SWE
12 products (Tedesco and Narvekar, 2010). Since the snowpack are usually rather unstable, it is awfully
13 unreasonable to set the snow density in the whole snow season to a constant. Observations show that
14 snow density does evolve and tends to increase ~~(decrease)~~ throughout the snow season (from September
15 to June) (Dai et al., 2012; Sturm et al., 1995). Here, daily snow density is obtained following Sturm et
16 al.(2010) (Eq. 3). They used daily SD, day of the year (DOY), and the snow climate class (SC) to produce
17 snowpack bulk density estimates. In this method, knowledge of SC is used to capture field environment
18 variables (air temperature, initial density) that have a considerable effect on snow density evolution.

$$\rho(SD, DOY, SC) = (\rho_{max} - \rho_0)[1 - \exp(-k_1 \times SD - k_2 \times DOY)] + \rho_0 \quad (3)$$

19 where ρ_{max} is the maximum density, ρ_0 is the initial density, k_1 and k_2 are densification parameters
20 for SD and DOY, respectively. k_1 , k_2 , ρ_{max} , ρ_0 vary with SC (Table 3). For operational purposes in
21 ~~our~~ [this](#) work, DOY extend to 1 September each year (Matthew Sturm, personal communication, 2018)
22 running from -122 (1 September) to 181 (30 June). Sturm et al. (2010) didn't compute snow density for
23 the SC ~~of~~ [as](#) ephemeral snow despite its presence in the Northern Hemisphere. According to Zhong et al.
24 (2014) study, the snow density of ephemeral is set to an fixed value, 0.25 g/cm³. Finally, daily snow
25 density is simulated by the Eq. 3 in the Northern Hemisphere during the 1992–2016 period.

1 4 Results and Discussion

2 4.1 Snow depth

3 4.1.1 Validation of snow depth

4 Here to give insight into relative performance of SD products, we compared three sources of snow
5 cover product (NHSnow, GlobSnow, and ERA-Interim/Land) with ground SD observations (Fig. 5-7)
6 using three indices bias, mean absolute error (MAE) and root mean square error (RMSE). The common
7 period (1992 - 2010) daily SD of three products (Section 2.4) were collected as validation data. This
8 validation work primarily focus on snow cover stabilization stage (December to February). Since the
9 snow density change slowly over a smaller range in snow cover stabilization stage (Xiao et al., 2018),
10 using a constant value (0.24 g/cm³) for GlobSnow could introduce relative little error (Section 3.3).
11 Subject to the unavailability of SWE station observations, the evaluation of SWE can't be carried out.

12 The relatively little bias (blue and green dots) between the estimated SD from three products against
13 measured SD is located in mid and low latitude regions (< 60 °N) for these three ~~snow depth~~SD datasets
14 (NHSnow, GlobSnow, and ERA-Interim/Land; Fig. 5). However, a large bias was found in the polar
15 region and along the coast, such as ~~the north of~~Russian coastal regions ~~near the Arctic Ocean~~, Russian
16 Far East, Korean peninsula, Northern Mediterranean and Northeast Canada. For NHSnow and GlobSnow,
17 most bias is distributed near the $\mu=0$ line with high frequency, although some bias is greater than 100 cm
18 (or less than -100 cm) (Fig. 5b, d). Positive (negative) biases indicate mean grid cell values less (greater)
19 than those of the respective stations SD measures. ~~Fig. 5c showed the~~ERA-Interim/Land overestimated d
20 snow depth in Western Siberian Plains and Eastern European Plains (around 60 °N; Fig. 5c, orange dots).
21 As reference, ~~Average~~average SD pattern of three products in February (1992-2010) were also provided
22 in Appendix (Fig. A)

23 For analysis indexes, MAE and RMSE, the distribution of error points of NHSnow and GlobSnow
24 are much the same as the distribution of its bias (Fig. 5-7). We used all evaluation records to calculate
25 three precision indexes for three products. We found that the bias, MAE and RMSE is 0.59 cm, 15.12 cm
26 and 20.11 cm, respectively, for NHSnow gridded products, ~~but~~ But for GlobSnow, there are more bias
27 (1.19 cm), MAE (15.98 cm) and lower RMSE (15.48 cm) ~~for GlobSnow~~ (Table 4). This comparison
28 (NHSnow vs. GlobSnow) showed relatively good agreement, although NHSnow over- or underestimated

1 the SD with larger RMSE. Overall, the performance of GlobSnow was better than the NHSnow gridded
2 product. However, part of the validation data were also applied for GlobSnow assimilation, it is highly
3 possible that in this case GlobSnow validation may not completely independent. The different
4 performance for these two products may be mainly because the evolution of snow grain size by HUT
5 (The Helsinki University of Technology) model was used to generate SWE in GlobSnow. Che et al. (2016)
6 reported that the grain size is more important than snow density and temperature. Further, ERA-
7 Interim/Land had the worst performance of all three products with highest bias (-5.60), MAE (18.72) and
8 RMSE (37.77). The smallest bias is located near mid-latitude regions ($< 50^\circ\text{N}$) and much of the bias lies
9 at 0–100 cm for ERA-Interim/Land products (Fig. 5e, f). It must be noted that there are 89 bias records
10 in two stations, which located in Novosibirsk Islands and Victoria Island, is much less than -300 cm
11 (approximately -3000 cm). Large MAE and RMSE can be found in high latitude and coastal region (Fig.
12 5e). Unlike NHSnow and GlobSnow, ERA-Interim/Land is more likely to overestimate SD and appears
13 to be less consistent with in situ observation across the Northern Hemisphere (Fig. 5f). Through analyzing
14 ground observation, we can see that deep snow is distributed in high latitude areas.

15 While the gridded products do a fairly good job of representing smaller accumulations of SD
16 (shallow and mid-deep snow cover), they all struggle to capture very high accumulations (deep snow)
17 with less bias, MAE and RMSE (Fig. 5-7, Fig. A). As a result, variation in snow cover could fail to be
18 adequately captured in areas with frequent deep snow and, thus, we should be cautious when interpreting
19 of this validation result.

20 Uncertainties in these three gridded snow products caused by ground temperature and topographic
21 factor could result in some level discrepancies between the measured and the estimated SD (Vander Jagt
22 et al., 2013; Snauffer et al., 2016). Forests exhibit strong influence on snow distributions by canopy
23 interception and the evolution of snow properties. The dense portions of boreal forests are widely
24 distributed in [NA North America](#) and northern [EU Eurasia](#) (Friedl et al., 2010) Large bias, MAE and
25 RMSE regions of three gridded products (Fig. 5-7) cover vast areas of tall vegetation (forests and shrub).
26 Furthermore, the spatial inhomogeneity cause s one grid cells (~25 km) that is almost not possible to
27 completely cover by one vegetation type (low heterogeneity). Because the estimated SD of NHSnow
28 depends on land cover types, this discrepancy induced by surface cover heterogeneity could partly
29 account for why NHSnow has a smaller MAE and RMSE for low vegetation (bare-land and prairie)
30 distributed at middle and low latitudes, than the higher vegetation (shrub and forest) areas at higher

1 latitudes (Xiao et al., 2018).

2 As well, there are scale mismatches between in situ observation and the gridded products with regard
3 to snowpack properties and their spatiotemporal representativeness (Frei et al., 2012). It is difficult to
4 precisely validate coarse-resolution satellite observation using ground truth. Subsequently, over- or
5 underestimates are inevitable when using a single in situ (SD or SWE) observation to test the veracity of
6 the gridded products (Mudryk et al., 2015; Xiao et al., 2018). Snow surveys would benefit from multiple
7 measurements at different points within one pixel (López-Moreno et al., 2011). In situ observations are
8 highly representative when the SD varies smoothly in space, and poorly representative when the SD is
9 spatially stepped (Che et al., 2016). However, there is almost always a lack of sufficient ground-measured
10 data. To date, field site observations are still to be more authentic and reliable datasets than satellite
11 observation.

12 As a whole, the accuracy of estimated SD in the Northern Hemisphere presented a spatial
13 heterogeneity. Issues of scale and spatial heterogeneity of validation data notwithstanding, these
14 comparisons conducted in our work can yield valuable insight into the performance of these products.

15 **4.1.2 Variation of snow depth**

16 To better understand and interpret snow cover variation across the Northern Hemisphere, we
17 conducted an analysis of SD variation using seasonal maximum SD from 1992–2016. According to the
18 rules of variation level grading, which was divided into 5 grade (extremely significant ~~decrease~~increase,
19 significant ~~decrease~~increase, non-significant change, ~~extremely~~significant ~~increase~~decrease, and
20 ~~extremely~~significant ~~increase~~decrease; Table 5), we can easily gained seasonal maximum SD variation
21 level range 1992 to 2016. Figure 8 shows the variation pattern of seasonal maximum SD in three seasons
22 (fall, winter and spring) with statistical significance level. In three seasons, variation trend of seasonal
23 maximum SD exhibited a distinctly different pattern over the Northern Hemisphere since 1992. Seasonal
24 maximum SD variation results in fall illustrated that a reduction trend account for most area of the
25 ~~EU~~Eurasia with the rate ranging from 0 to 1 cm yr⁻¹. The Figure 8a shows the significant level pattern
26 of corresponding maximum SD change trend. We can find that the area, which show extremely significant
27 decrease in fall, are mainly located in the Russian Far East, the Qinghai-Tibet Plateau, the southern
28 Siberian Plateau, and the northeastern region of Canada. On the contrary, Russia's Taimyr Peninsula and

1 the United States' Alaska region shows extremely significant increase trend ($0 \sim 1 \text{ cm yr}^{-1}$). In addition,
2 the maximum SD in winter and spring also exhibited extremely significant decrease in the Qinghai-Tibet
3 Plateau and the northeastern region of Canada (~~as shown in~~ Figure 8b and 8c). The area with extremely
4 significant decrease ~~trend extend to~~ add a Western Siberian plain region. Wang and Li (2012) used nearly
5 50a of daily station SD observation data to analyze the trend of maximum SD in China. The variation
6 trend of seasonal maximum SD in the Qinghai-Tibet Plateau ~~from~~ Wang and Li (2012) ~~previous study~~
7 is consistent with the conclusion observed in this study (~~Wang and Li, 2012~~). There are more regions in
8 seasonal maximum SD with extremely significant increase trend in winter and spring (green region).
9 Furthermore, ~~a strange phenomenon that~~ the variations ~~trend~~ of seasonal maximum SD in the Russian
10 Far East show ~~an~~ extremely significant decrease, while ~~in spring, it showed an extremely significant~~
11 ~~increase~~ ~~it is in inverse in spring~~. This variation trend of maximum SD in spring analyzed using NHSnow
12 products is consistent with the analysis results using GlobSnow products ~~from recently published study~~
13 (Wu et al., 2018). ~~It need be pointed out that the significant increase (decrease) area is located around~~
14 ~~extremely significant increase (decrease) as shown in Figure 8. No matter which season, although the~~
15 ~~variation trend of maximum seasonal SD didn't pass the significance level test, we can draw the~~
16 ~~conclusion that the wide range of area across the Northern Hemisphere experienced pronounced change~~
17 ~~during the period 1992 to 2016.~~

18 Finally, we analyzed seasonal ~~variation analysis~~ variation ~~of~~ SD across the Northern Hemisphere using
19 seasonal average SD ~~as analysis index~~. Seasonal average SD was defined as the cumulative SD divided
20 by the days in one snow cover season (~~refer to Eq. A in Appendix~~). SD variation rate fluctuated in
21 different regions and seasons. It was generally large in the region north of 55° N (Fig. 9, Fig. B and C in
22 appendix). This fluctuation was large in winter with high of $-0.11 \pm 0.40 \text{ cm yr}^{-1}$ than other seasons
23 during 1992–2016 (Fig. 9d, Table 6.), which ~~means~~ ~~implies~~ that the maximum changes ~~in average SD~~
24 occurred in winter. Similar conclusion also can be easily found in the two periods 1992–2001 and 2002–
25 2016 (Fig. B-d, C-d and Table 6). Although not all variation trends passed the significance test, most
26 regions in the Northern Hemisphere show increasing trends during 1992-2001 (Fig. B; Table 6). The SD
27 variation trend in the three seasons during 2002–2016 was reversed. The ~~SD~~ absolute variation rate
28 during 2002–2016 is apparently greater than ~~its rate that~~ during 1992–2001 (Fig. C; Table 6). ~~The last~~
29 ~~century were considered to be the warmest period.~~

30 The high fluctuation of SD variation rate especially occurred in the ~~polar region (the a~~ Arctic and

1 the Qinghai-Tibetan plateau) for three seasons. ~~In the context of global climate change, we found that~~
2 ~~winter SD variation was more sensitive to climate change. The strength of this relationship is spatially~~
3 ~~complex, varying by latitude, region, and climate condition.~~

4 4.2 Snow mass

5 GlobSnow dataset covers all land surface areas excluding mountainous regions, glaciers and
6 Greenland ~~as described in Section 2.4~~. From above analysis, we ~~can find~~ that ERA-Interim/Land have
7 somewhat poor performance in SD estimation. ~~Thus, f~~urther analysis of snow cover variation in the
8 Northern Hemisphere used NHSnow products as analysis data. ~~The forecast for snow mass have great~~
9 ~~potential consequences on agriculture practices in many regions.~~ Snow mass ~~in here~~ is calculated by
10 SWE multiplied by snow cover area (Qin et al., 2006). It should be noted that the snow classification tree
11 (Grody and Basist, 1996), which have been applied in many studies (Che et al., 2008; Dai et al., 2017; Yu
12 et al., 2012), was used to detect snow cover for NHSnow product. Liu et al. (2018) also reported that
13 Grody's algorithm had higher positive predictive values and lower omission errors by testing snow cover
14 mapping algorithms with the in situ SD over China. In this study, Monthly average snow mass, aAnnual
15 ~~(or monthly~~ maximum, average, and minimum in one snow cover year from September 1 through June
16 30 were calculated in 25 years, which is the sum of daily (or the mean of monthly) total SWE in one
17 ~~snow cover year (or each month of 25 years).~~

18 The snow mass variation characteristic over the past 25 years were explored by iInterannual
19 variation (Fig. 10) and intra-annual cycles (not show figure) of ~~total SWE~~snow mass over the Northern
20 Hemisphere ~~were used to analyze total SWE variation characteristic over the past 25 years (1992–2016)~~.
21 Figure 10 ~~8~~ depicts the time series of interannual variation of annual ~~total SWE~~maximum, average and
22 minimum snow mass anomaly with respect to 1992–2016 ~~reference~~-period. The biggest value of annual
23 maximum snow mass anomaly occurred in 1998–1999 up to 4875 km³ period, with while the least
24 minimum was 3969 km³ in during 2007-20082015–2016. ~~It~~ The annual maximum snow mass present
25 particularly significant decreasing trends ($P \leq 0.05$) during 1992–2016, at the rate of approximately -
26 ~~5794~~19.88 km³ yr.⁻¹ (Fig. 10A). Trend analysis reveals that annual maximum ~~total SWE~~snow mass
27 have a 8~~12.5~~% reduction from 1992 to 2016. Note that it~~There is present~~ a slow-increase variation trend
28 ~~rate~~ by about ~~710~~25.59 km³ yr.⁻¹ ($P > 0.05$)rate for 1992-2001 ~~period~~. In contrast, the annual maximum
29 total SWEsnow mass exhibits a anomaly significantly decrease trends (with -34.80 km³ yr.⁻¹, $P \leq 0.05$)

1 ~~after since 2002 at rate of approximately 9041 km³ yr⁻¹~~, which ~~may~~ would lead to a extraordinary
2 decreasing trends of total SWE during 1992–2016. According to the static, the annual maximum snow
3 mass usually appear in February (about 60%) and March (about 40%), and in recent several years this
4 occurred in March become a normal state~~here was a sudden drop of total SWE in 2008–2009 as found~~
5 ~~in previous studies~~. This finding needs to be further analyzed in the future work by correlation with
6 climatic factors, such as precipitation effects (Kumar et al., 2012). We find that the biggest and the least
7 value of annual average snow mass respectively appear in 1998-1999 (~2370 km³) and 2015-2016
8 (~1850 km³) in Fig 10B. Likewise, in Fig 10B and 10C the annual average (minimum) snow mass
9 exhibit a significant decrease trend in 1992-2016 period by rate -19.72 km³ yr⁻¹, P > 0.05 (-2.00 km³
10 yr⁻¹, P < 0.05) and 2002-2016 period at a rate of -30.70 km³ yr⁻¹, P > 0.05 (-2.2 km³ yr⁻¹, P < 0.05). For
11 1992-2016 period, the variation tendency of annual average (minimum) snow mass do not pass the
12 significance level test. Moreover, the reduction for the annual average and annual minimum snow mass
13 is 13% and 67%, respectively. However, ~~o~~Other factors, for instance, oceanic and atmospheric heat
14 transport, sea ice season wind, and solar insolation anomalies, may have contributed to the fluctuation
15 of ~~total SWE~~snow mass (Liu and Key, 2014). Variation of ~~total SWE~~snow mass across the Northern
16 Hemisphere could well capture the variation characteristic of the Arctic sea ice extent (Tilling et al.,
17 2015).

18 When analyzing long-term variation of monthly average ~~total SWE~~snow mass (refer to Eq. B in
19 Appendix), ten months (September to June) exhibit significant decreasing apart from March and April
20 (Table 7). The maximum decrease rate was approximately ~~-1066~~-36.50 km³ yr⁻¹ (P < 0.05) in ~~January~~
21 November while the minimum decrease occurred in ~~September-April~~ at ~~-4.29~~-1.77 km³ yr⁻¹ (P > 0.05).
22 However, there are no significant trends in March and April with large interannual variations (Table
23 7). An increasing trend appears in March with a rate of approximately 68 km³ yr⁻¹ (P > 0.05), however,
24 ~~relatively large decrement in fall and winter are unable to partially be offset by the increment of March.~~
25 Compared with the fall (September to November) and spring (~~February-March~~ to June), the interannual
26 variability of monthly average ~~total SWE~~snow mass significantly decreased in winter (December to
27 ~~January-February~~), with average rate of less than ~~-32~~-10.00 km³ yr⁻¹. The reduction of monthly average
28 snow mass in ten month were generated using the average pattern of each month over 1992-2016 as a
29 reference. We ~~also~~ found that the reduction of monthly average ~~total SWE~~snow mass ~~reduction~~
30 fluctuated ranging from ~~-66~~-65% to -4% for each month (September to June) over 1992-2016 (Table 7).

1 The largest and smallest reduction were about ~~65.8~~4.67% and ~~4.302~~2%, which occurred in June and
2 March, respectively. [Variation analysis of monthly average snow mass could offer a powerful evidence](#)
3 [for annual average snow mass exhibit a significantly decreasing tendency \(Table 7, Fig. 10B\).](#)

4 ~~Over large areas, it is extremely convenient to use remote sensing to infer SWE. Albeit there are~~
5 ~~numerous ways to estimate SWE, it~~ is very challenging to determine precise distributions of SWE at
6 regional and global scales (Chang et al., 1987;Kongoli, 2004;Tedesco and Narvekar, 2010;Bair et al.,
7 2018). Snow density, which can be used to convert SWE from SD, is ~~potential~~ and key factor in accurate
8 estimation of SWE (Sturm et al., 2010;Tedesco and Narvekar, 2010). In fact, snow density typically
9 varies from 0.05 g/cm³ for ~~new~~fresh snow at low air temperatures to over 0.55 g/cm³ for a ripened
10 snowpack (Anderton et al., 2004;Cordisco et al., 2006). Noteworthy, this study ~~uses~~using dynamic snow
11 density to convert SD to SWE ~~is based on~~with the assumption that snowpack occurs as a single layer
12 (Sturm et al., 2010), ~~to capture dynamic characteristics of snow property~~. The evolution of the ephemeral
13 snow class ~~was~~did not be provided by Sturm et al. (2010). The mean value (0.25 g/cm³) of snow density
14 of ephemeral snow (Zhong et al., 2014), which means ~~that~~ without any evolution throughout the snow
15 cover year. Meanwhile, ~~this value for ephemeral snow was set as 0.2275 g/cm³ in~~ Tedesco and Jeyaratnam
16 (2016) [used snow density of 0.2275 g/cm³ for ephemeral snow, which is about 10% lower than the value](#)
17 [used in this study](#)~~study~~. Snow density also exhibits great heterogeneity in vertical direction, so that a
18 single layer of snow concept cannot fully capture the snowpack property. The density ~~at~~of the top of
19 snowpack (fresh snow; ~ 0.10 g/cm³) increases gradually ~~downwards from the top toward the bottom~~
20 (Dai et al., 2012). The bottom layer of snowpack is old snow undergoing compaction and grain size
21 growth with a relatively high density (0.3~0.6 g/cm³). ~~Although our snow density description strategy~~
22 ~~does not completely describe the actual evolution in snow density, there is no better alternative.~~

23 4.3 Snow cover days

24 Snow cover days (SCD) is defined as the number of days in one snow cover year in which SD is
25 over 0 cm (Zhong, 2014). Snow cover year was defined as the period between the July 1 of a given year
26 and the June of the following year (Xiao et al., 2018). A least-squares regression was used to analyze the
27 variation of SCD for each pixel from 24 snow cover years, with per-pixel evaluation of significance (F-
28 test).

29 We ~~exploring~~investigated the changes and variation in SCD during 1992-2016. Most areas across

1 the Northern Hemisphere present a prominently decreasing trend at a rate ranging ~~from~~ 0 to 5 day yr.⁻¹
2 (Fig. 11a). Decreasing regions are mainly distributed in ~~EU~~[Eurasia](#). For example, north of Russia and
3 large parts of central Asia. The area that shows decreasing trends of SCD in ~~EU~~[Eurasia](#) is much larger
4 than that in ~~NA~~[North America](#) (Fig. 11a) (Derksen and Brown, 2012). Areas that the decrease at a rate
5 greater than 5 day yr.⁻¹ are almost all located in China, such as North of Qilian Mountain, central Tibetan
6 Plateau, and Tianshan Mountain. Areas ~~that exhibits~~[with](#) increasing trends, can be found in central of
7 ~~NA~~[North America](#), Western Europe, Northwestern Mongolia, and some parts of China. Throughout the
8 Northern Hemisphere (Fig. 11b), the decreasing trend covered most parts of the regions (~~25 through~~
9 ~~85 °N~~) with a mean decreasing rate of approximately 1.0 day yr.⁻¹. ~~Latitudes~~[Regions](#) around 50 °N is an
10 exception [almost with no changes](#)~~where variation is close to 0 day yr.⁻¹~~. The most notable variation trend
11 (decreasing or increasing) occurred over polar regions (Fig. 11b). This may be because there are few
12 pixels in the polar mainland.

13 ~~SCD variation rate also were divided into 5 grade (Table 5).~~ Unlike SCD variation rate patterns, the
14 variation level pattern shows that the non-significant changes area dominates SCD variation trends across
15 the Northern Hemisphere (Fig. 11c). Extremely significant and significant decrease appear in northwest
16 of Hudson Bay in Canada, Kamchatka peninsula, Eastern European plains, the north of Russia, Iranian
17 plateau, and several regions in China (the Tibet Plateau, Tianshan Mountain and Northeast China Plain).
18 In addition, extremely significant and significant increase only occur in a limited area of ~~NA~~[North](#)
19 [America](#), eastern [Qinghai-Tibetan](#) Plateau regions, and China's central and northern regions.

20 Interestingly, the opposite variation trends in SCD and SD appear in several regions. Maximum SD
21 in spring (Fig. 8c) and annual average SD (figure not shown) show extremely significant increasing
22 trends, whereas SCD exhibit extremely significant decreases in corresponding regions (Fig. 11c), such
23 as Central Siberian Plateau, Greater Khingan Mountains in China, and the eastern Scandinavian
24 Peninsula. This different variation trend of SD and SCD was also reported by Zhong et al. (2018) using
25 ground-based data. The primary reason may be the increase of frequency of extreme snowfall in which
26 SD could demonstrate on increasing trend. Additionally, a recent study found that the greater SWE, the
27 faster melting rate leading to a shortened SCD in Northern Hemisphere (Wu et al., 2018).

28 Despite the similarities between the station- and satellite-derived time series, it can be demonstrated
29 that Northern Hemisphere meteorological station data do not provide perfect large-scale variation
30 characteristics of ground snow cover (Zhong et al., 2018). Our analyses provide further evidence

1 supporting observations of significant decreasing trends in SCD occurring in the Northern Hemisphere.
2 Compared to SCD derived from optic sensors snow cover product, however, the specific quantity of SCD
3 and SCD variation rate derived from NHSnow SD data was overestimated (Wang et al., 2018;Hori et al.,
4 2017). The SCD variation trends derived from NHSnow product ~~almost~~ is [about the](#) same as [one](#) derived
5 from optical snow cover product in variation pattern (Hori et al., 2017).

6 Since the optical (MODIS or AVHRR) and microwave sensors (SSM/I or AMSR-E) respond in
7 different parts of the electromagnetic spectrum, the estimated snow cover will to be somewhat vary. The
8 shallow snow could not induce volume scattering at 37 GHz, and thus passive microwave observations
9 often ~~give~~ [provide](#) better snow cover result at thick snow (>5 cm) (Foster et al., 2009;Wang et al., 2008).
10 The threshold for SCD definition ~~in~~ here is 0 cm, whereas it is 1 cm or larger in other studies (Ke et al.,
11 2016;Dyer and Mote, 2006). As well, another explanation for these discrepancy could be snow cover
12 identification algorithm (Liu et al., 2018;Hall et al., 2002).

13 The microwave radiation characteristics of snow cover is similar to that of precipitation, cold desert
14 and, frozen ground (Grody and Basist, 1996). Commission and omission errors in NHSnow product may
15 result from coarse spatial resolution, snow characteristics and topography according to Dai et al. (2017),
16 precipitation (Liu et al., 2018;Grody and Basist, 1996) especially over frozen ground (Tsutsui and Koike,
17 2012). ~~Algorithm s~~ Several rules [for NHSnow algorithm development](#) were ~~applied~~
18 from precipitation, cold desert, and frozen ground (Xiao et al., 2018), it is impossible to entirely remove
19 interference factors in each image. Additionally, the precondition of NHSnow is dry snow, which mean
20 almost no wet snow was considered into SCD variation analysis (Singh and Gan, 2000). The poorer
21 performance of the microwave derived products was anticipated because of documented difficulties
22 monitoring snow cover over forested and mountainous terrain (Vander Jagt et al., 2013;Smith and
23 Bookhagen, 2016).

24 **5 Conclusions**

25 This ~~project~~ [study](#) applied the SVR ~~SD-snow-depth~~ retrieval algorithm ~~proposed~~ [developed](#) by Xiao
26 et al (2018), which using PM remote sensing and other auxiliary data, to ~~develop~~ [generate](#) a long term
27 ~~(from~~ January [1](#), 1992 to December [31](#), 2016) Northern Hemisphere daily SD and SWE products
28 (NHSnow) with 25-km spatial resolution. We then analyzed the spatial and temporal change in snow

1 cover (SD, ~~total SWE~~[snow mass](#) and, SCD) across the Northern Hemisphere, and quantified the
2 magnitude of variation of snow cover using SD and SWE extracted from NHSnow product.

3 In this study, we validated ~~three and compared among~~ daily gridded products (NHSnow, GlobSnow
4 and ERA-Interim/Land) against ground [truth](#) snow-depth ~~measurements~~[observations](#). The results show
5 ~~relatively~~ high estimation accuracy of SD from NHSnow, providing the relatively little bias, RMSE, and
6 MAE ~~between the newly SD products and in situ observation. Analysis of~~ SD variation revealed that the
7 variation rates ranging from ~~0-1~~ to 1 cm yr.⁻¹ ~~(negative and positive)~~ dominates the change in the
8 Northern Hemisphere, and the maximum changes appear in winter. Additionally, the results revealed [that](#)
9 the overall SD trends in three seasons show increasing trend during 1992–2001, however it has a
10 decreasing trend during 2002–2016. Similar conclusions also appear in ~~total SWE~~[snow mass](#) change
11 analysis. The ~~total SWE~~[annual maximum, average and minimum snow mass exhibit significantly](#)
12 [decrease trends and respectively](#) shows a ~~8%, 132.5% and 67%~~ reduction, ~~and~~ [The monthly average](#)
13 [snow mass has shown a decreasing trend almost in every month](#) ~~onthly average total SWE and the~~
14 [reduction range from is 64.67](#)~~65.8% (June) to for the largest reduction and a 4.32% (March) for least~~
15 ~~reduction which occur in June and March, respectively.~~ The ~~total SWE~~[annual average snow mass](#) report
16 well-documented significant decreasing trends (~~~20 km³ yr.⁻¹~~, P < 0.05) during the study period.
17 Regression analysis multi-year Northern Hemisphere SCD exhibits a prominent decreasing trend at a
18 rate ranging from 0 to 5 day yr.⁻¹. The area of decreasing trends of SCD in ~~EU~~[Eurasia](#) is much larger than
19 in ~~NA~~[North America](#). Unlike the SCD variation rate, its variation level shows that non-significant
20 changes areas dominate the variation pattern across the Northern Hemisphere. An abnormal and
21 interesting phenomenon is that opposite SCD and SD variation trends appear in several regions.

22 While this study shed light on the spatiotemporal variability trends of snow cover across the
23 Northern Hemisphere using 25-year NHSnow product, we cannot claim NHSnow dataset could
24 completely capture the climate change signal in each region and season. Because of the deficiencies and
25 limitations (e.g. overestimation, underestimation), further efforts should be made to improve the
26 estimation accuracy and robustness of the SD inversion algorithm. Additionally, when more reliable and
27 numerous data become available, we will do more comprehensive validation over higher latitudes and
28 mountainous regions (Dai et al., 2017). Meanwhile, the validation analysis also should be carried out in
29 complex terrain and different land cover types (Tennant et al., 2017; Snauffer et al., 2016). It is
30 recommended that future work focus on the climatic effects and climatological causes in snow cover

1 changes to comprehensively understand the associated snow cover change mechanisms against a climate
 2 change background (Huang et al., 2017;Flanner et al., 2011;Cohen et al., 2012).

3 Acknowledgments

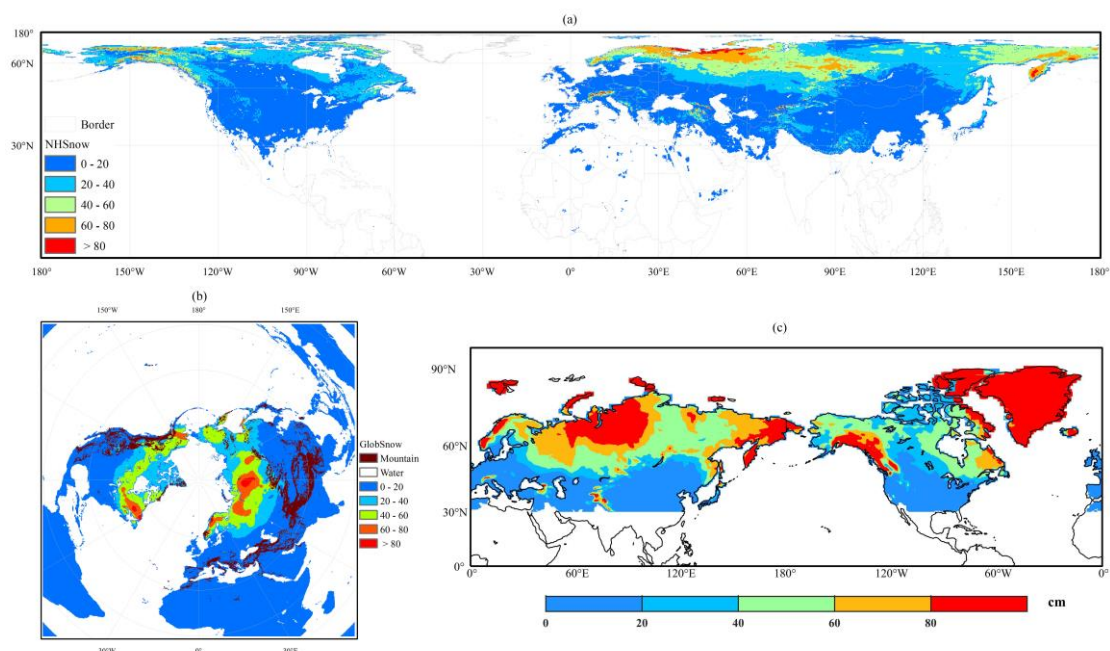
4 This study was funded by the National Natural Science Foundation of China (grant nos. 91325202;
 5 41871050; 41801028), National Key Scientific Research Program of China (grant no. 2013CBA01802),
 6 and the Strategic Priority Research Program of Chinese Academy of Sciences (grant nos. XDA20100103;
 7 XDA20100313).

8 Appendix

$$SD_{average} = \frac{\sum_{i=1}^n SD_i}{n} \quad (A)$$

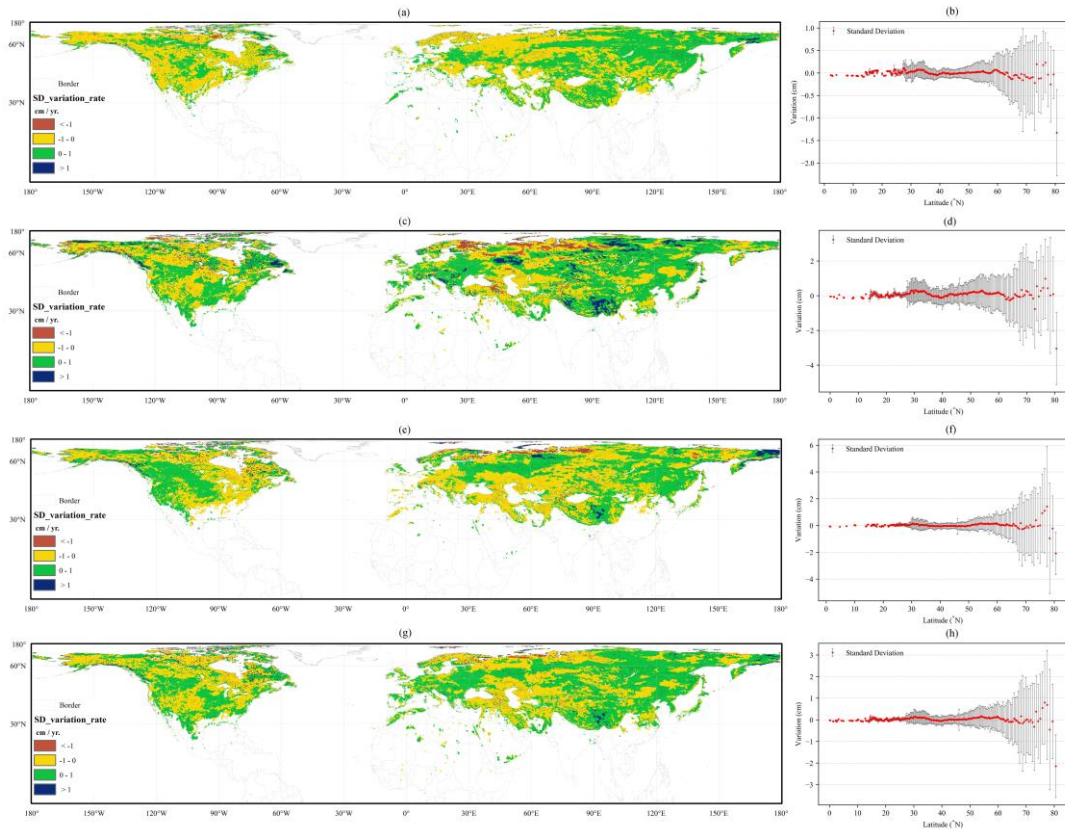
$$SM_{average} = \frac{\sum_{i=1}^n SM_i}{n} \quad (B)$$

9 Where n is the number of days in one specific period of time (one month, or snow cover year/season),
 10 i is i th day in one specific period of time (one month, or snow cover year/season). SD is snow depth.
 11 SM is snow mass.



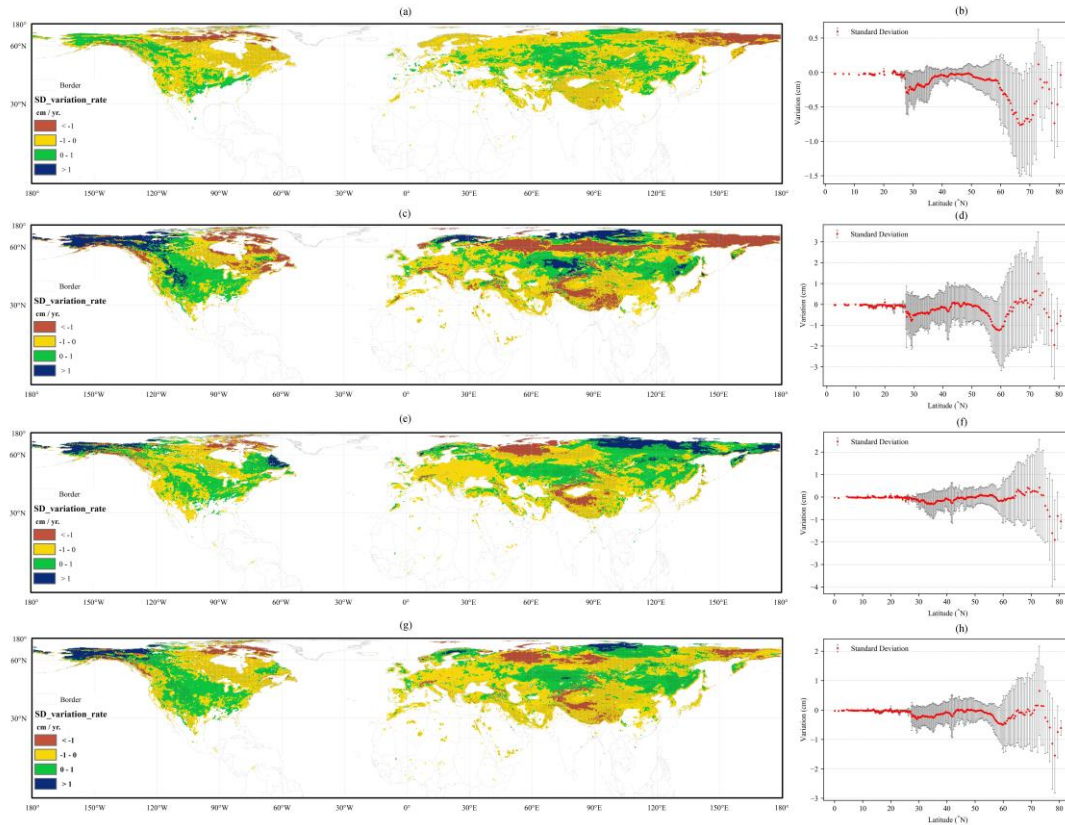
12
 13 Figure A. Monthly average snow depth climatology of three products in February during 1992-2010: a)
 14 NHSnow; b) GlobSnow, c) ERA-Interim/Land

1



2

3 Figure B. The variation rate pattern of annual average (season) SD over the Northern Hemisphere for
4 three snow cover season, fall (a, b; September to November), winter (c, d; December to February),
5 spring (e, f; March to June) from 1992-2001. Black dots in (a, c, e, g) indicate that the changes are
6 significant at 95% confidence level (CL). The zonal distribution in (b, d, f, h) are mapped at 0.25
7 degree resolution in latitude. The error bars in (b, d, f, h) is one times of standard deviation.



1
2
3
4
5
6
7

Figure C. The variation rate pattern of annual (season) average SD over the Northern Hemisphere for three snow cover season, fall (a, b; September to November), winter (c, d; December to February), spring (e, f; March to June) from 2002-2016. Black dots in (a, c, e, g) indicate that the changes are significant at 95% confidence level (CL). The zonal distribution in (b, d, f, h) are mapped at 0.25 degree resolution in latitude. The error bars in (b, d, f, h) is one times of standard deviation.

1

Table A. AVHRR Global Land Cover classification and reclassification schemes

Value	Classification Label	Reclassification Label
0	Water	Water
1	Evergreen needle leaf forest	Forest
2	Evergreen broad leaf forest	
3	Deciduous needle leaf forest	
4	Deciduous broad leaf forest	
5	Mixed forest	
6	Woodland	
7	Wooded grassland	
10	Grassland	
8	Closed shrub land	Shrub
9	Open shrub land	
11	Cropland	Bare-land
12	Bare ground	
13	Urban and built	

2

1 References

- 2 Amante, C., Eakins, B.W.: ETOPO1 1 arc-minute global relief model: procedures, data sources and
3 analysis, US Department of Commerce, National Oceanic and Atmospheric Administration, National
4 Environmental Satellite, Data, and Information Service, National Geophysical Data Center, Marine
5 Geology and Geophysics Division Colorado, 2009.
- 6 Anderton, S. P., White, S. M., and Alvera, B.: Evaluation of spatial variability in snow water equivalent
7 for a high mountain catchment, *Hydrological Processes*, 18, 435-453, 10.1002/hyp.1319, 2004.
- 8 Armstrong, R., and Brodzik, M.: An earth-gridded SSM/I data set for cryospheric studies and global
9 change monitoring, *Advances in Space Research*, 16, 155-163, 1995.
- 10 Armstrong, R. L., Knowles, K. W., Brodzik, M.J., Hardman, M.A.: DMSP SSM/I pathfinder daily EASE-
11 grid brightness temperatures, Boulder, Colorado USA: National snow and ice data center, Digital media,
12 2008.
- 13 Bair, E. H., Andre Calfa, A., Rittger, K., and Dozier, J.: Using machine learning for real-time estimates
14 of snow water equivalent in the watersheds of Afghanistan, *The Cryosphere*, 12, 1579-1594, 10.5194/tc-
15 12-1579-2018, 2018.
- 16 Balsamo, G., Albergel, C., Beljaars, A., Boussetta, S., Brun, E., Cloke, H., Dee, D., Dutra, E., Munoz-
17 Sabater, J., and Papenberger, F.: ERA-Interim/Land: A global land surface reanalysis dataset, *European*
18 *Geosciences Union General Assembly*, 2015, 389-407,
- 19 Barnett, T. P., Adam, J. C., and Lettenmaier, D. P.: Potential impacts of a warming climate on water
20 availability in snow-dominated regions, *Nature*, 438, 303-309, 10.1038/nature04141, 2005.
- 21 Barrett, B. S., Henderson, G. R., and Werling, J. S.: The Influence of the MJO on the Intraseasonal
22 Variability of Northern Hemisphere Spring Snow Depth, *Journal of Climate*, 28, 7250-7262, 10.1175/jcli-
23 d-15-0092.1, 2015.
- 24 Bilello, M. A.: Regional and seasonal variations in snow-cover density in the U.S.S.R, 1984.
- 25 Brodzik, M. J., and Knowles, K.: EASE-Grid: A Versatile Set of Equal-Area Projections and Grids, 2002.
- 26 Brown, R., Derksen, C., and Wang, L.: A multi-data set analysis of variability and change in Arctic spring
27 snow cover extent, 1967–2008, *Journal of Geophysical Research*, 115, 10.1029/2010jd013975, 2010.
- 28 Brown, R., and Robinson, D.: Northern Hemisphere spring snow cover variability and change over 1922–
29 2010 including an assessment of uncertainty, *The Cryosphere*, 5, 219-229, 2011.
- 30 Brown, R. D., and Frei, A.: Comment on “Evaluation of surface albedo and snow cover in AR4 coupled
31 models” by A. Roesch, *Journal of Geophysical Research*, 112, 10.1029/2006jd008339, 2007.
- 32 Chang, A., Foster, J., and Hall, D.: Nimbus-7 SMMR derived global snow cover parameters, *Ann. Glaciol*,
33 9, 39-44, 1987.
- 34 Che, T., Xin, L., Jin, R., Armstrong, R., and Zhang, T.: Snow depth derived from passive microwave
35 remote-sensing data in China, *Annals of Glaciology*, 49, 145-154, 2008.
- 36 Che, T., Dai, L., Zheng, X., Li, X., and Zhao, K.: Estimation of snow depth from passive microwave
37 brightness temperature data in forest regions of northeast China, *Remote Sensing of Environment*, 183,
38 334-349, 2016.
- 39 Cohen, J. L., Furtado, J. C., Barlow, M. A., Alexeev, V. A., and Cherry, J. E.: Arctic warming, increasing
40 snow cover and widespread boreal winter cooling, *Environmental Research Letters*, 7, 10.1088/1748-
41 9326/7/1/014007, 2012.
- 42 Cordisco, E., Prigent, C., and Aires, F.: Snow characterization at a global scale with passive microwave
43 satellite observations, *Journal of Geophysical Research*, 111, 10.1029/2005jd006773, 2006.
- 44 Dai, L., Che, T., Wang, J., and Zhang, P.: Snow depth and snow water equivalent estimation from AMSR-

1 E data based on a priori snow characteristics in Xinjiang, China, *Remote Sensing of Environment*, 127,
2 14-29, 2012.

3 Dai, L., Che, T., and Ding, Y.: Inter-calibrating SMMR, SSM/I and SSMI/S data to improve the
4 consistency of snow-depth products in China, *Remote Sensing*, 7, 7212-7230, 2015.

5 Dai, L., Che, T., Ding, Y., and Hao, X.: Evaluation of snow cover and snow depth on the Qinghai–Tibetan
6 Plateau derived from passive microwave remote sensing, *The Cryosphere*, 11, 1933-1948, 10.5194/tc-
7 11-1933-2017, 2017.

8 Derksen, C., Walker, A., and Goodison, B.: Evaluation of passive microwave snow water equivalent
9 retrievals across the boreal forest/tundra transition of western Canada, *Remote Sensing of Environment*,
10 96, 315-327, 2005.

11 Derksen, C., and Brown, R.: Spring snow cover extent reductions in the 2008-2012 period exceeding
12 climate model projections, *Geophysical Research Letters*, 39, n/a-n/a, 10.1029/2012gl053387, 2012.

13 Diffenbaugh, N. S., Scherer, M., and Ashfaq, M.: Response of snow-dependent hydrologic extremes to
14 continued global warming, *Nat Clim Chang*, 3, 379-384, 10.1038/nclimate1732, 2013.

15 Dutra, E., Balsamo, G., Viterbo, P., Miranda, P. M. A., Beljaars, A., Schär, C., and Elder, K.: An improved
16 snow scheme for the ECMWF land surface model: description and offline validation, *Journal of*
17 *Hydrometeorology*, 11, 899-916, 2010.

18 Dyer, J. L., and Mote, T. L.: Spatial variability and trends in observed snow depth over North America,
19 *Geophysical Research Letters*, 33, 10.1029/2006gl027258, 2006.

20 Flanner, M. G., Shell, K. M., Barlage, M., Perovich, D. K., and Tschudi, M. A.: Radiative forcing and
21 albedo feedback from the Northern Hemisphere cryosphere between 1979 and 2008, *Nature Geoscience*,
22 4, 151-155, 10.1038/ngeo1062, 2011.

23 Forman, B. A., Reichle, R. H., and Derksen, C.: Estimating Passive Microwave Brightness Temperature
24 Over Snow-Covered Land in North America Using a Land Surface Model and an Artificial Neural
25 Network, *IEEE Transactions on Geoscience & Remote Sensing*, 52, 235-248, 2013.

26 Forman, B. A., and Reichle, R. H.: Using a support vector machine and a land surface model to estimate
27 large-scale passive microwave brightness temperatures over snow-covered land in North America, *IEEE*
28 *Journal of Selected Topics in Applied Earth Observations and Remote Sensing*, 8, 4431-4441, 2015.

29 Foster, J., Chang, A., and Hall, D.: Comparison of snow mass estimates from a prototype passive
30 microwave snow algorithm, a revised algorithm and a snow depth climatology, *Remote sensing of*
31 *environment*, 62, 132-142, 1997.

32 Foster, J. L., Hall, D. K., Kelly, R. E. J., and Chiu, L.: Seasonal snow extent and snow mass in South
33 America using SMMR and SSM/I passive microwave data (1979–2006), *Remote Sensing of*
34 *Environment*, 113, 291-305, 10.1016/j.rse.2008.09.010, 2009.

35 Foster, J. L., Hall, D. K., Eylander, J. B., Riggs, G. A., Nghiem, S. V., Tedesco, M., Kim, E., Montesano,
36 P. M., Kelly, R. E. J., Casey, K. A., and Choudhury, B.: A blended global snow product using visible,
37 passive microwave and scatterometer satellite data, *International Journal of Remote Sensing*, 32, 1371-
38 1395, 10.1080/01431160903548013, 2011.

39 Frei, A., Tedesco, M., Lee, S., Foster, J., Hall, D. K., Kelly, R., and Robinson, D. A.: A review of global
40 satellite-derived snow products, *Advances in Space Research*, 50, 1007-1029, 10.1016/j.asr.2011.12.021,
41 2012.

42 Friedl, M. A., Sulla-Menashe, D., Tan, B., Schneider, A., Ramankutty, N., Sibley, A., and Huang, X.:
43 MODIS Collection 5 global land cover: Algorithm refinements and characterization of new datasets,
44 *Remote Sensing of Environment*, 114, 168-182, 2010.

1 Friedl, M. A., and Sulla-Menashe, D.: Note to users of MODIS Land Cover (MCD12Q1) Products,
2 Report. Accessed March, 2, 2014, 2011.

3 Gan, T. Y., Barry, R. G., Gizaw, M., Gobena, A., and Balaji, R.: Changes in North American snowpacks
4 for 1979–2007 detected from the snow water equivalent data of SMMR and SSM/I passive microwave
5 and related climatic factors, *Journal of Geophysical Research: Atmospheres*, 118, 7682-7697, 2013.

6 Gharaei-Manesh, S., Fathzadeh, A., and Taghizadeh-Mehrjardi, R.: Comparison of artificial neural
7 network and decision tree models in estimating spatial distribution of snow depth in a semi-arid region
8 of Iran, *Cold Regions Science and Technology*, 122, 26-35, 2016.

9 Goïta, K., Walker, A. E., and Goodison, B. E.: Algorithm development for the estimation of snow water
10 equivalent in the boreal forest using passive microwave data, *International Journal of Remote Sensing*,
11 24, 1097-1102, 2003.

12 Grippa, M., Mognard, N., Le Toan, T., and Josberger, E.: Siberia snow depth climatology derived from
13 SSM/I data using a combined dynamic and static algorithm, *Remote sensing of environment*, 93, 30-41,
14 2004.

15 Grody, N. C., and Basist, A. N.: Global identification of snowcover using SSM/I measurements, *IEEE*
16 *Transactions on geoscience and remote sensing*, 34, 237-249, 1996.

17 Hall, D. K., Kelly, R. E. J., Riggs, G. A., Chang, A. T. C., and Foster, J. L.: Assessment of the relative
18 accuracy of hemispheric-scale snow-cover maps, *Annals of Glaciology*, 34, 24-30, 2002.

19 Hancock, S., Baxter, R., Evans, J., and Huntley, B.: Evaluating global snow water equivalent products
20 for testing land surface models, *Remote sensing of environment*, 128, 107-117,
21 10.1016/j.rse.2012.10.004, 2013.

22 Hansen, M. C., Defries, R. S., Townshend, J. R. G., and Sohlberg, R.: Global land cover classification at
23 1 km spatial resolution using a classification tree approach, *International Journal of Remote Sensing*, 21,
24 1331-1364, 2000.

25 Hori, M., Sugiura, K., Kobayashi, K., Aoki, T., Tanikawa, T., Kuchiki, K., Niwano, M., and Enomoto,
26 H.: A 38-year (1978–2015) Northern Hemisphere daily snow cover extent product derived using
27 consistent objective criteria from satellite-borne optical sensors, *Remote Sensing of Environment*, 191,
28 402-418, 10.1016/j.rse.2017.01.023, 2017.

29 Huang, X., Deng, J., Ma, X., Wang, Y., Feng, Q., Hao, X., and Liang, T.: Spatiotemporal dynamics of
30 snow cover based on multi-source remote sensing data in China, *The Cryosphere*, 10, 2453-2463,
31 10.5194/tc-10-2453-2016, 2016.

32 Huang, X., Deng, J., Wang, W., Feng, Q., and Liang, T.: Impact of climate and elevation on snow cover
33 using integrated remote sensing snow products in Tibetan Plateau, *Remote Sensing of Environment*, 190,
34 274-288, 10.1016/j.rse.2016.12.028, 2017.

35 Immerzeel, W. W., Van Beek, L. P., and Bierkens, M. F.: Climate Change Will Affect the Asian Water
36 Towers, *Science*, 328, 1382-1385, 2010.

37 Ke, C.-Q., Li, X.-C., Xie, H., Ma, D.-H., Liu, X., and Kou, C.: Variability in snow cover phenology in
38 China from 1952 to 2010, *Hydrology and Earth System Sciences*, 20, 755-770, 10.5194/hess-20-755-
39 2016, 2016.

40 Kongoli, C.: Interpretation of AMSU microwave measurements for the retrievals of snow water
41 equivalent and snow depth, *Journal of Geophysical Research*, 109, 10.1029/2004jd004836, 2004.

42 Kumar, M., Wang, R., and Link, T. E.: Effects of more extreme precipitation regimes on maximum
43 seasonal snow water equivalent, *Geophysical Research Letters*, 39, 10.1029/2012gl052972, 2012.

44 Li, W., Guo, W., Qiu, B., Xue, Y., Hsu, P. C., and Wei, J.: Influence of Tibetan Plateau snow cover on

1 East Asian atmospheric circulation at medium-range time scales, *Nat Commun*, 9, 4243,
2 10.1038/s41467-018-06762-5, 2018.

3 Liang, J., Liu, X., Huang, K., Li, X., Shi, X., Chen, Y., and Li, J.: Improved snow depth retrieval by
4 integrating microwave brightness temperature and visible/infrared reflectance, *Remote Sensing of*
5 *Environment*, 156, 500-509, 2015.

6 Liu, X., Jiang, L., Wu, S., Hao, S., Wang, G., and Yang, J.: Assessment of Methods for Passive Microwave
7 Snow Cover Mapping Using FY-3C/MWRI Data in China, *Remote Sensing*, 10, 10.3390/rs10040524,
8 2018.

9 Liu, Y., and Key, J. R.: Less winter cloud aids summer 2013 Arctic sea ice return from 2012 minimum,
10 *Environmental Research Letters*, 9, 10.1088/1748-9326/9/4/044002, 2014.

11 López-Moreno, J. I., Fassnacht, S. R., Beguería, S., and Latron, J. B. P.: Variability of snow depth at the
12 plot scale: implications for mean depth estimation and sampling strategies, *The Cryosphere*, 5, 617-629,
13 10.5194/tc-5-617-2011, 2011.

14 Mudryk, L. R., Derksen, C., Kushner, P. J., and Brown, R.: Characterization of Northern Hemisphere
15 Snow Water Equivalent Datasets, 1981–2010, *Journal of Climate*, 28, 8037-8051, 10.1175/jcli-d-15-
16 0229.1, 2015.

17 Pulliainen, J.: Mapping of snow water equivalent and snow depth in boreal and sub-arctic zones by
18 assimilating space-borne microwave radiometer data and ground-based observations, *Remote Sensing of*
19 *Environment*, 101, 257-269, 2006.

20 Qin, D., Liu, S., and Li, P.: Snow cover distribution, variability, and response to climate change in western
21 China, *J. Climate*, 19, 1820-1833, 2006.

22 Robinson, D. A., and Frei, A.: Seasonal variability of Northern Hemisphere snow extent using visible
23 satellite data, *The Professional Geographer*, 52, 307-315, 2000.

24 Rupp, D. E., Mote, P. W., Bindoff, N. L., Stott, P. A., and Robinson, D. A.: Detection and Attribution of
25 Observed Changes in Northern Hemisphere Spring Snow Cover, *Journal of Climate*, 26, 6904-6914,
26 10.1175/jcli-d-12-00563.1, 2013.

27 Singh, P. R., and Gan, T. Y.: Retrieval of snow water equivalent using passive microwave brightness
28 temperature data, *Remote Sensing of Environment*, 74, 275-286, 2000.

29 Smith, T., and Bookhagen, B.: Assessing uncertainty and sensor biases in passive microwave data across
30 High Mountain Asia, *Remote Sensing of Environment*, 181, 174-185, 2016.

31 Snauffer, A. M., Hsieh, W. W., and Cannon, A. J.: Comparison of gridded snow water equivalent products
32 with in situ measurements in British Columbia, Canada, *Journal of Hydrology*, 541, 714-726,
33 10.1016/j.jhydrol.2016.07.027, 2016.

34 Sturm, M., Holmgren, J., and Liston, G. E.: A seasonal snow cover classification system for local to
35 global applications, *Journal of Climate*, 8, 1261-1283, 1995.

36 Sturm, M., Taras, B., Liston, G. E., Derksen, C., Jonas, T., and Lea, J.: Estimating snow water equivalent
37 using snow depth data and climate classes, *Journal of Hydrometeorology*, 11, 1380-1394, 2010.

38 Sturm, M.: White water: Fifty years of snow research in WRR and the outlook for the future, *Water*
39 *Resources Research*, 51, 4948-4965, 10.1002/2015wr017242, 2015.

40 Takala, M., Luojus, K., Pulliainen, J., Derksen, C., Lemmetyinen, J., Kärnä, J.-P., Koskinen, J., and
41 Bojkov, B.: Estimating northern hemisphere snow water equivalent for climate research through
42 assimilation of space-borne radiometer data and ground-based measurements, *Remote Sensing of*
43 *Environment*, 115, 3517-3529, 2011.

44 Tedesco, M., Pulliainen, J., Takala, M., Hallikainen, M., and Pampaloni, P.: Artificial neural network-

1 based techniques for the retrieval of SWE and snow depth from SSM/I data, *Remote sensing of*
2 *Environment*, 90, 76-85, 2004.

3 Tedesco, M., and Narvekar, P. S.: Assessment of the NASA AMSR-E SWE Product, *IEEE Journal of*
4 *Selected Topics in Applied Earth Observations and Remote Sensing*, 3, 141-159, 2010.

5 Tedesco, M., Derksen, C., Deems, J. S., and Foster, J. L.: Remote sensing of snow depth and snow water
6 equivalent, *Remote Sensing of the Cryosphere*, 73-98, 2014.

7 Tedesco, M., and Jeyaratnam, J.: A New Operational Snow Retrieval Algorithm Applied to Historical
8 AMSR-E Brightness Temperatures, *Remote Sensing*, 8, 2016.

9 Tennant, C. J., Harpold, A. A., Lohse, K. A., Godsey, S. E., Crosby, B. T., Larsen, L. G., Brooks, P. D.,
10 Kirk, R. W. V., and Glenn, N. F.: Regional sensitivities of seasonal snowpack to elevation, aspect, and
11 vegetation cover in western North America, *Water Resources Research*, 53, 2017.

12 Tilling, R. L., Ridout, A., Shepherd, A., and Wingham, D. J.: Increased Arctic sea ice volume after
13 anomalously low melting in 2013, *Nature Geoscience*, 8, 643-646, 10.1038/ngeo2489, 2015.

14 Tsutsui, H., and Koike, T.: Development of Snow Retrieval Algorithm Using AMSR-E for the BJ
15 Ground-Based Station on Seasonally Frozen Ground at Low Altitude on the Tibetan Plateau, *Journal of*
16 *the Meteorological Society of Japan. Ser. II*, 90C, 99-112, 10.2151/jmsj.2012-C07, 2012.

17 Vander Jagt, B. J., Durand, M. T., Margulis, S. A., Kim, E. J., and Molotch, N. P.: The effect of spatial
18 variability on the sensitivity of passive microwave measurements to snow water equivalent, *Remote*
19 *Sensing of Environment*, 136, 163-179, 2013.

20 Wang, C., and Li, D.: Spatial-temporal variations of snow cover days and the maximum depth of snow
21 cover in China during recent 50 years, *Journal of Glaciology and Geocryology*, 34, 247-256, 2012.

22 Wang, X., Xie, H., and Liang, T.: Evaluation of MODIS snow cover and cloud mask and its application
23 in Northern Xinjiang, China, *Remote Sensing of Environment*, 112, 1497-1513,
24 10.1016/j.rse.2007.05.016, 2008.

25 Wang, Y., Huang, X., Liang, H., Sun, Y., Feng, Q., and Liang, T.: Tracking Snow Variations in the
26 Northern Hemisphere Using Multi-Source Remote Sensing Data (2000–2015), *Remote Sensing*, 10,
27 10.3390/rs10010136, 2018.

28 Wegmann, M., Orsolini, Y., Dutra, E., Bulygina, O., Sterin, A., and Brönnimann, S.: Eurasian snow depth
29 in long-term climate reanalyses, *The Cryosphere*, 11, 923-935, 10.5194/tc-11-923-2017, 2017.

30 Wentz, F. J.: SSM/I version-7 calibration report, *Remote Sensing Systems Tech. Rep.*, 11012, 46, 2013.

31 Wu, X., Che, T., Li, X., Wang, N., and Yang, X.: Slower Snowmelt in Spring Along With Climate
32 Warming Across the Northern Hemisphere, *Geophysical Research Letters*, 45, 12,331-312,339,
33 10.1029/2018gl079511, 2018.

34 Xiao, X., Zhang, T., Zhong, X., Shao, W., and Li, X.: Support vector regression snow-depth retrieval
35 algorithm using passive microwave remote sensing data, *Remote Sensing of Environment*, 210, 48–64,
36 2018.

37 Xu, X., Liu, X., Li, X., Xin, Q., Chen, Y., Shi, Q., and Ai, B.: Global snow cover estimation with
38 Microwave Brightness Temperature measurements and one-class in situ observations, *Remote Sensing*
39 *of Environment*, 182, 227-251, 2016.

40 Xue, Y., and Forman, B. A.: Comparison of passive microwave brightness temperature prediction
41 sensitivities over snow-covered land in North America using machine learning algorithms and the
42 Advanced Microwave Scanning Radiometer, *Remote Sensing of Environment*, 170, 153-165, 2015.

43 Ye, H., Cho, H.-r., and Gustafson, P. E.: changes in russian winter snow accumulation during 1936-83
44 and its spatial patterns, *Journal of Climate*, 11, 856-863, 1998.

- 1 Yu, H., Zhang, X., Liang, T., Xie, H., Wang, X., Feng, Q., and Chen, Q.: A new approach of dynamic
2 monitoring of 5 - day snow cover extent and snow depth based on MODIS and AMSR - E data from
3 Northern Xinjiang region, *Hydrological Processes*, 26, 3052-3061, 2012.
- 4 Zhang, T., Osterkamp, T., and Stamnes, K.: Influence of the depth hoar layer of the seasonal snow cover
5 on the ground thermal regime, *Water Resources Research*, 32, 2075-2086, 1996.
- 6 Zhang, T.: Influence of the seasonal snow cover on the ground thermal regime: An overview, *Reviews of*
7 *Geophysics*, 43, 589-590, 2005.
- 8 Zhang, Y., Li, T., and Wang, B.: Decadal Change of the Spring Snow Depth over the Tibetan Plateau_
9 The Associated Circulation and Influence on the East Asian Summer Monsoon, *Journal of Climate*, 17,
10 2780-2793, 2004.
- 11 Zhong, X.: Spatiotemporal variability of snow cover and the relationship between snow and climate
12 change across the Eurasian Continent, Lanzhou: Cold and Arid Regions Environmental and Engineering
13 Research Institute, CAS, 2014.
- 14 Zhong, X., Zhang, T., and Wang, K.: Snow density climatology across the former USSR, *The Cryosphere*,
15 8, 785-799, 2014.
- 16 Zhong, X., Zhang, T., Kang, S., Wang, K., Zheng, L., Hu, Y., and Wang, H.: Spatiotemporal variability
17 of snow depth across the Eurasian continent from 1966 to 2012, *The Cryosphere*, 12, 227-245,
18 10.5194/tc-12-227-2018, 2018.
- 19

1 **List of Tables and Figures**

2 Table 1 Detail description for SSM/ and SSMIS sensors. H and V denotes horizontal and vertical
 3 polarization, respectively.

Satellite	SSM/I		SSMIS
Platform	F 11	F 13	F 17
Temporal coverage	1991.12-1995.5	1995.5-2008.6	2006.12 -
Channels (GHz)	19 H, V; 22 V; 37 H, V; 85 H, V		19 H, V; 22 V; 37 H, V; 91 H, V

4

5 Table 2. Training sample filter rules

Layer ID	Filter rules
Layer2.	$\text{If } \text{Number}_{total}(\text{layer2}) \leq 3000$ $\text{Number}_{training}(\text{layer2}) = (\text{Number}_{total}(\text{layer2}))/2$ $\text{Else } \text{Number}_{training}(\text{layer2}) = 3000$
Layer3.	$\text{If } \text{Number}_{total}(\text{layer3}) \leq 3000$ $\text{Number}_{training}(\text{layer3}) = (\text{Number}_{total}(\text{layer3}))/2$ $\text{Else } \text{Number}_{training}(\text{layer3}) = 3000$
Layer1.	$\text{If } \text{Number}_{training}(\text{layer2}) > 2000 \text{ or } \text{Number}_{training}(\text{layer3}) > 1000$ $\text{Number}_{training}(\text{layer1})$ $= 15000 - \text{Number}_{training}(\text{layer2}) - \text{Number}_{training}(\text{layer3})$ $\text{Else } \text{Number}_{training}(\text{layer1}) = 12000$

6

7 Table 3 Snow density estimation model parameters

Snow class	ρ_{max}	ρ_0	k_1	k_2	References
Alpine	0.5975	0.2237	0.0012	0.0038	Sturm et al. (2010)
Maritime	0.5979	0.2578	0.0010	0.0038	
Prairie	0.5940	0.2332	0.0016	0.0031	
Tundra	0.3630	0.2425	0.0029	0.0049	
Taiga	0.2170	0.2170	0	0	
Ephemeral	0.2500	0.2500	0	0	Zhong et al. (2014)

8

1 Table 4. The evaluated indexes (bias, MAE, RMSE; unit: cm) for three gridded SD products (NHSnow,
2 GlobSnow, ERA-Interim/Land).

Products	Bias	MAE	RMSE
NHSnow	0.59	15.12	20.11
GlobSnow	1.19	15.98	15.48
ERA-Interim/Land	-5.60	18.72	37.77

3

4 Table 5. Rules of variation level grading

Variation rate	P value	Variation level
rate $> \leq 0$	$p \leq 0.01$	extremely significant decrease increase
rate $> \leq 0$	$0.01 < p \leq 0.05$	significant increase decrease
-	$P > 0.05$	non-significant change
rate $< \geq 0$	$0.01 < p \leq 0.05$ $p \leq 0.01$	extremely significant increase decrease
rate $< \geq 0$	$0.01 < p \leq 0.05$ $p \leq 0.01$	extremely significant increase decrease

5

6 Table 6. Mean variation rate of average SD (cm yr.⁻¹) over the Northern Hemisphere for three common
7 period (1992-2016, 1992-2001, 2002-1996) and snow cover seasons (fall, winter, spring). Std. means
8 standard deviation

Season	1992-2016 (Mean \pm 1 Std.)	1992-2001 (Mean \pm 1 Std.)	2002-2016 (Mean \pm 1 Std.)
Fall	-0.08 \pm 0.11	-0.01 \pm 0.19	-0.15 \pm 0.22
Winter	-0.11 \pm 0.40	0.06 \pm 0.62	-0.22 \pm 0.75
Spring	-0.04 \pm 0.25	0.02 \pm 0.51	-0.07 \pm 0.41
Year	-0.06 \pm 0.20	0.02 \pm 0.35	-0.11 \pm 0.34

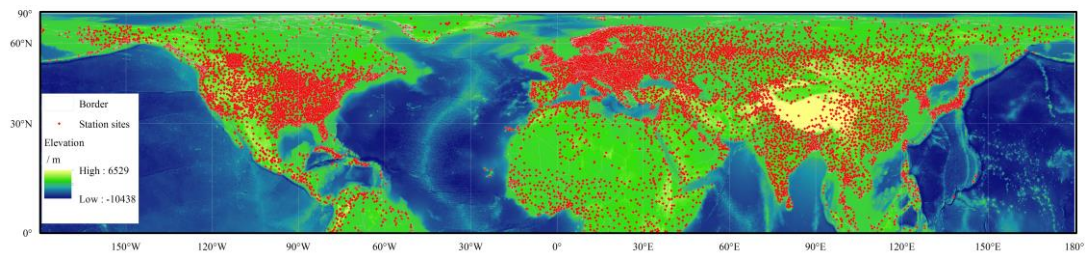
9

10 Table 7. Variation rate and changes of monthly average [snow mass during 1992-2016](#). The asterisk
11 indicate that the changes are significant at 95% confidence level. [The changes was calculated with](#)
12 [respect to the average of monthly average snow mass on 25 years.](#)

Month	Variation rate (km ³ /yr.)	The percentage of % Changes in the mean of monthly average over 1992-2016 period
September	<u>-5.96*</u>	<u>-63.89%</u>
October	<u>-25.50*</u>	<u>-43.99%</u>
November	<u>-36.50*</u>	<u>-26.96%</u>
December	<u>-32.66*</u>	<u>-5.00%</u>
January	<u>-34.38*</u>	<u>-9.53%</u>
February	<u>-30.89*</u>	<u>-11.91%</u>
March	<u>1.90</u>	<u>-4.30%</u>
April	<u>-4.29</u>	<u>-6.46%</u>
May	<u>-11.33*</u>	<u>-19.59%</u>
June	<u>-8.01*</u>	<u>-64.67%</u>

1

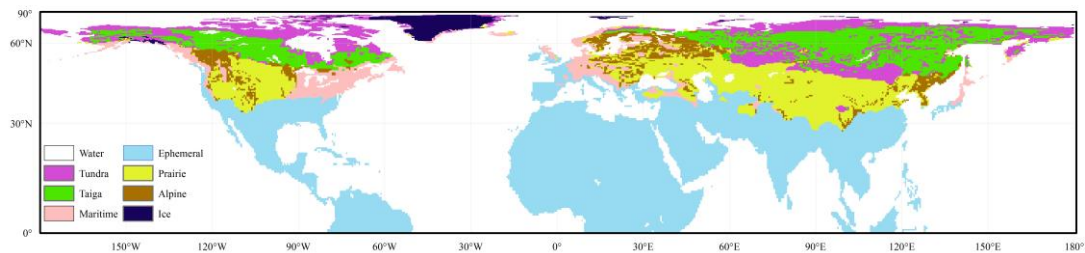
2



3

4 Figure 1. Distribution of Meteorological stations overlaid on ETOPO1 in the Northern Hemisphere.

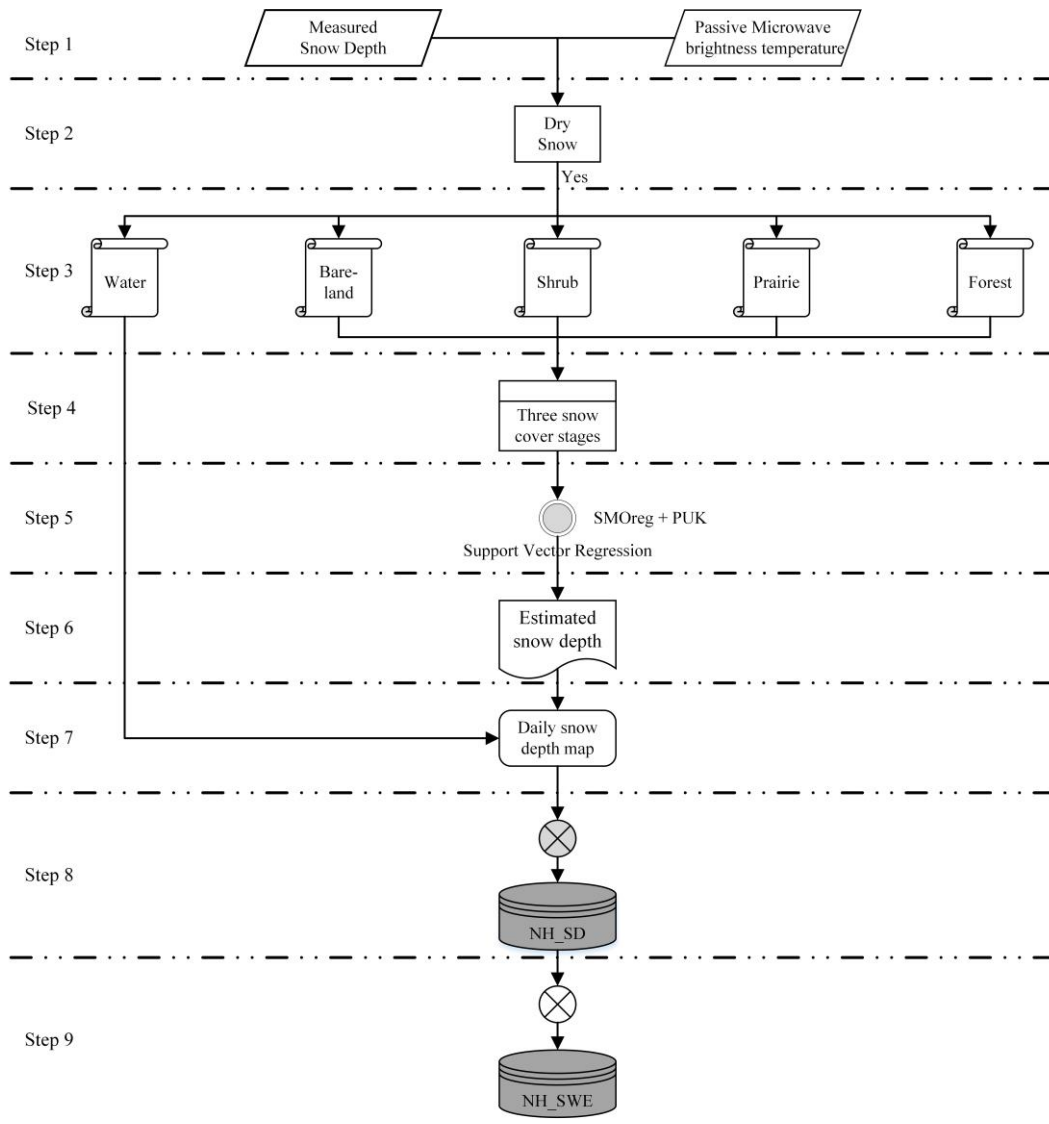
5



6

7

Figure 2. Snow Class distribution in the Northern Hemisphere



1
2
3
4
5

Figure 3. Process flowchart diagram for developing Northern Hemisphere daily snow depth and snow water equivalent data

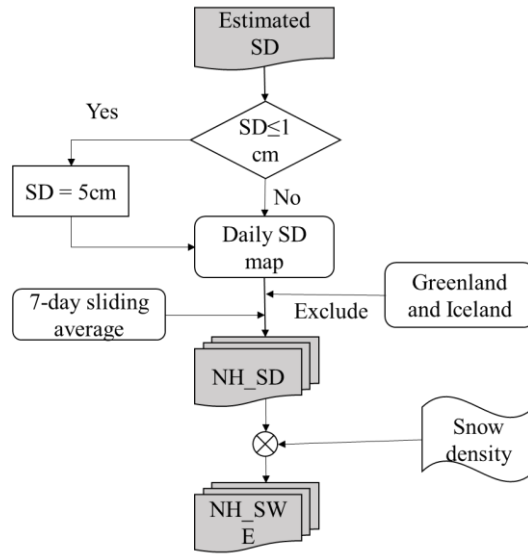


Figure 4. Flowchart diagram of the generation of NHSnow products.

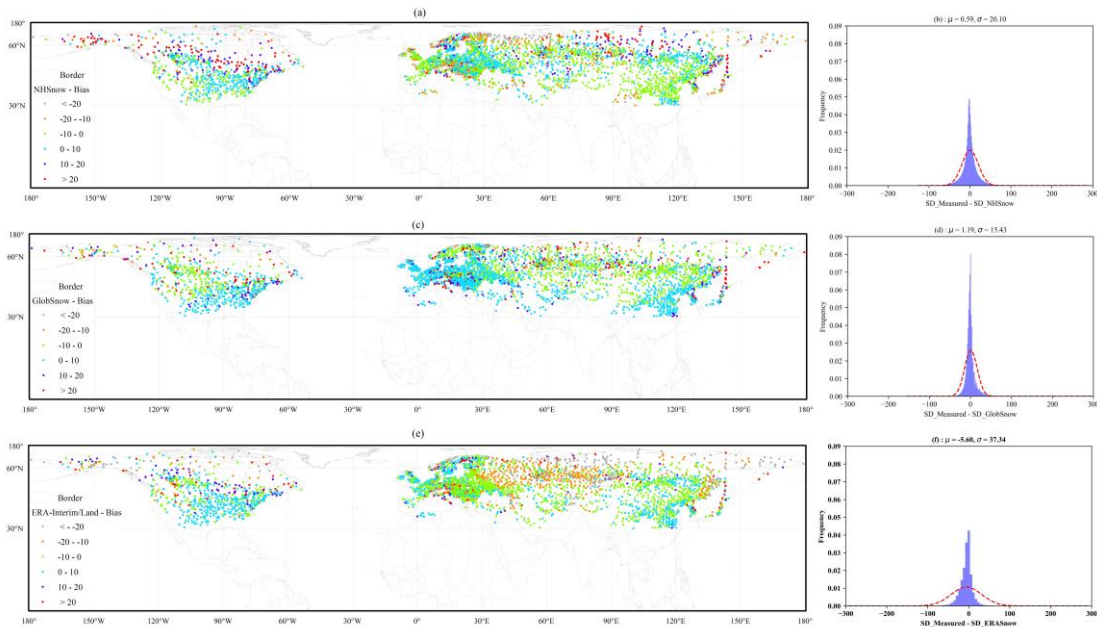
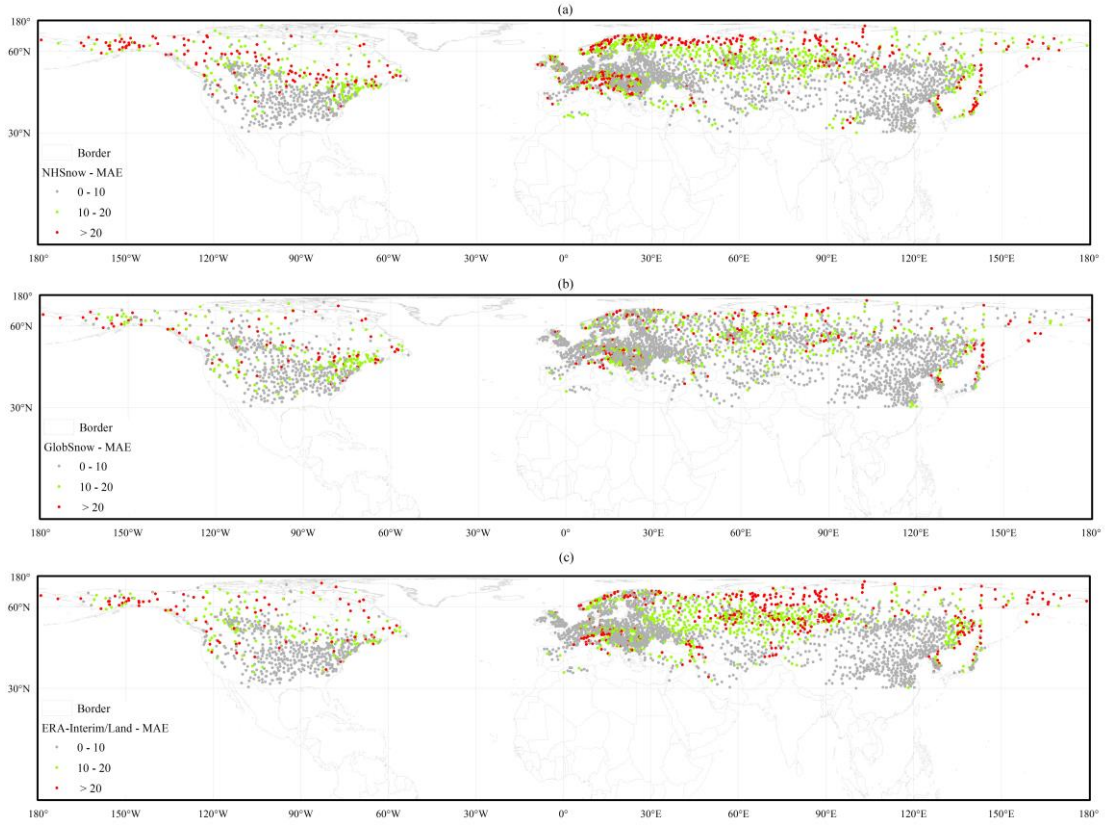
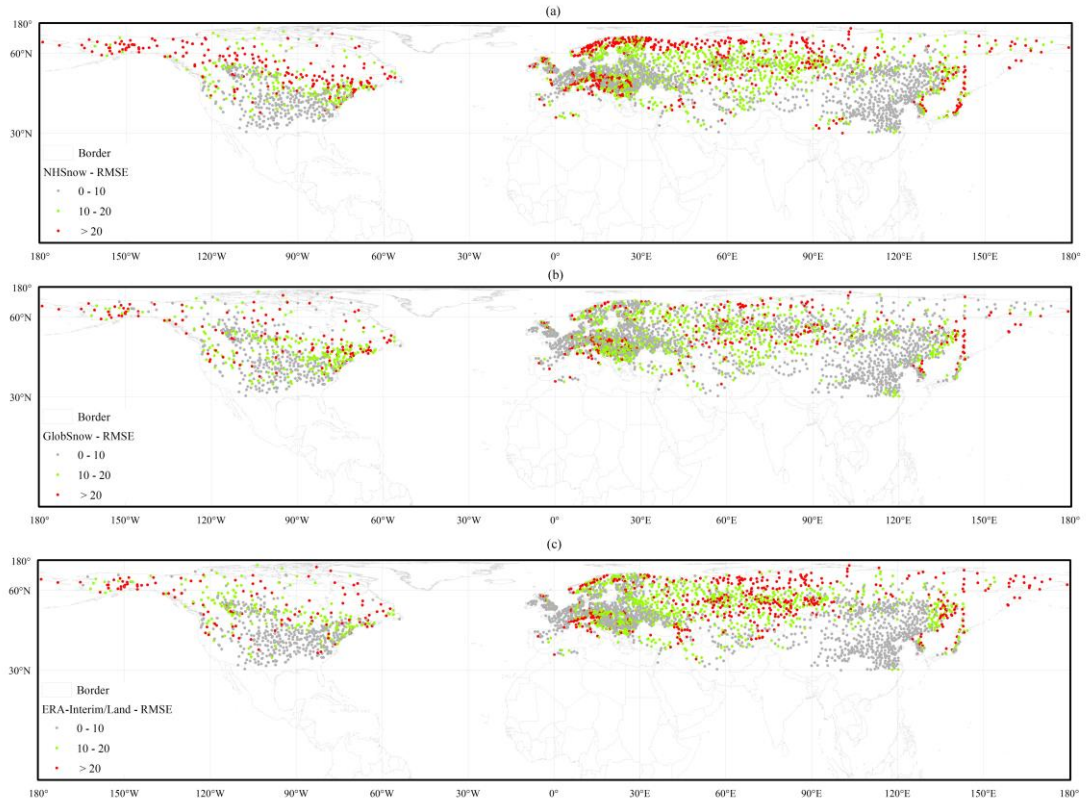


Figure 5. Bias of each meteorological station and histogram of biases for three products: a), b) NHSnow; c), d) GlobSnow, e), f) ERA-Interim/Land. The red dashed line in right column figures are the fitted normal distribution curve



1

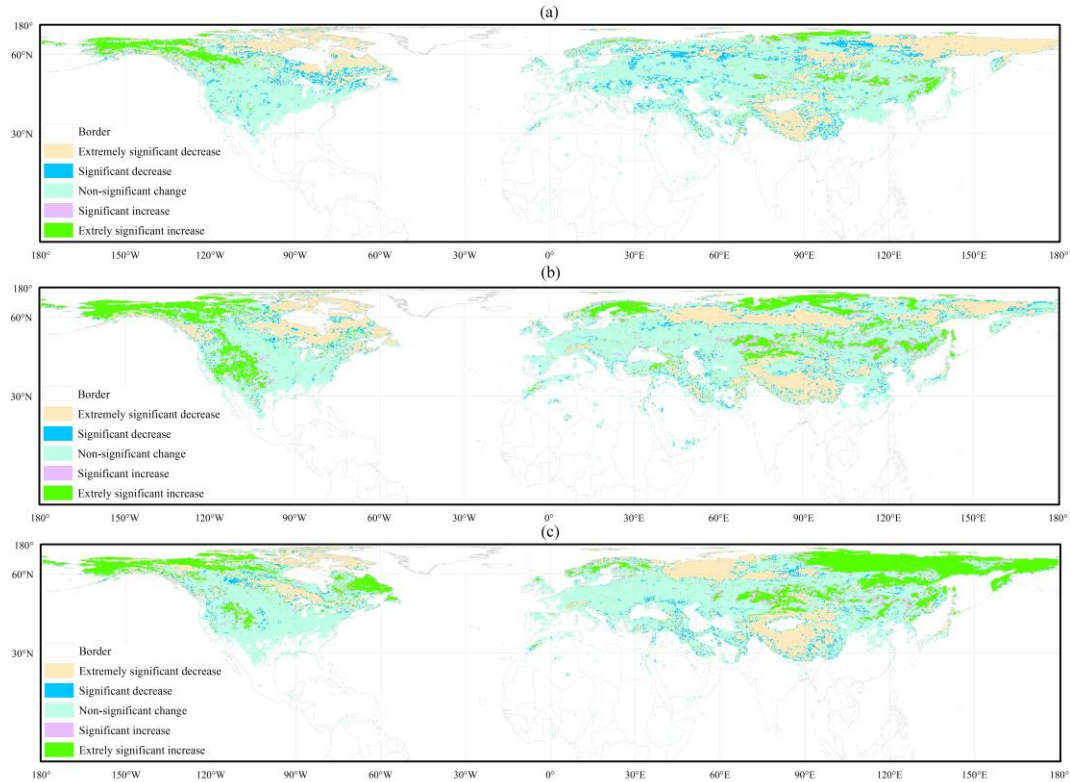
2 Figure 6. MAE of each meteorological station for three products: a) NHSnow, b) GlobSnow, c) ERA-
 3 Interim/Land.



4

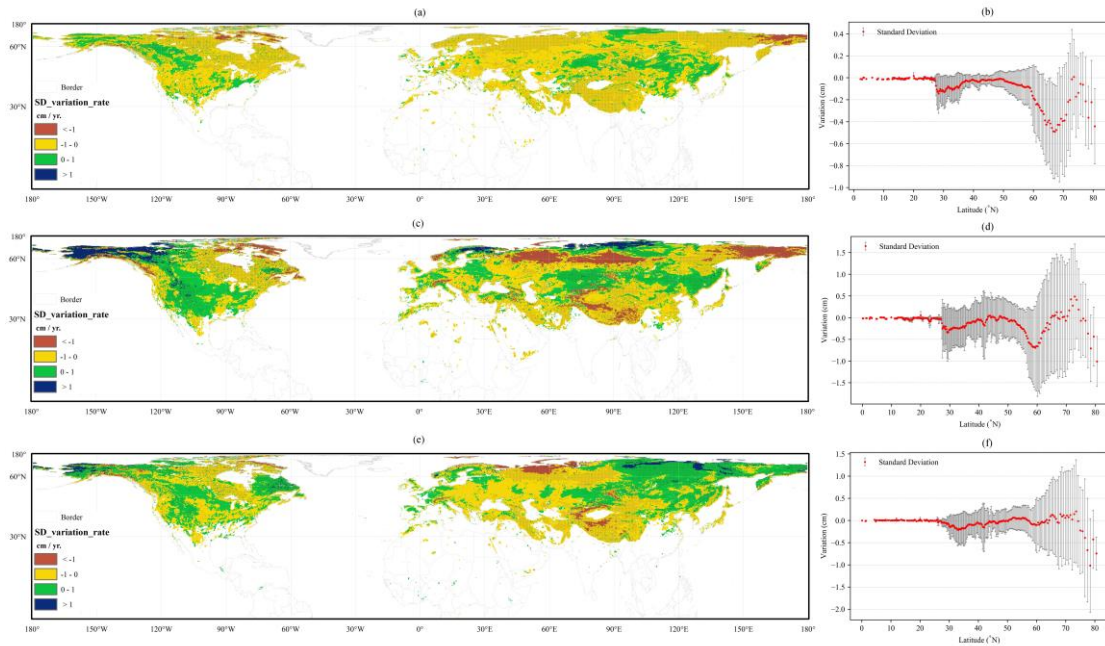
1 Figure 7. RMSE of each meteorological station for three products: a) NHSnow, b) GlobSnow, c) ERA-
2 Interim/Land.

3



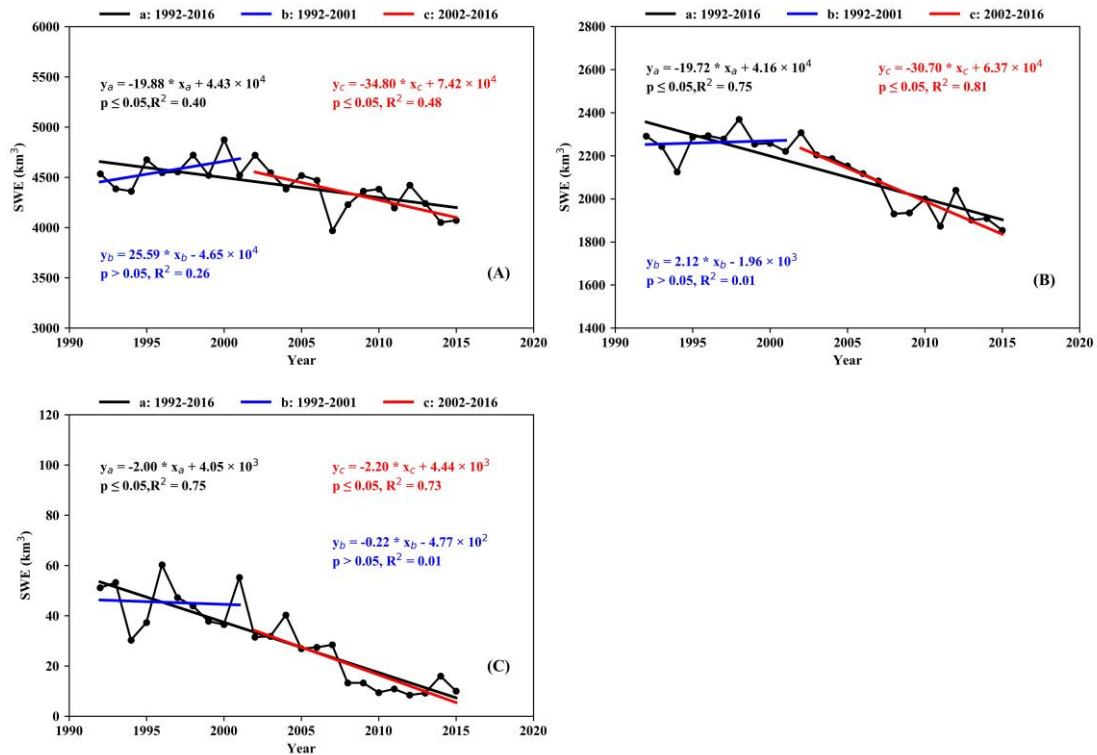
4

5 Figure 8. The variation rate pattern of season maximum SD with statistical significances over the
6 Northern Hemisphere for three snow cover season, fall (a; September to November), winter (b;
7 December to February), spring (c; March to June) from 1992-2016.



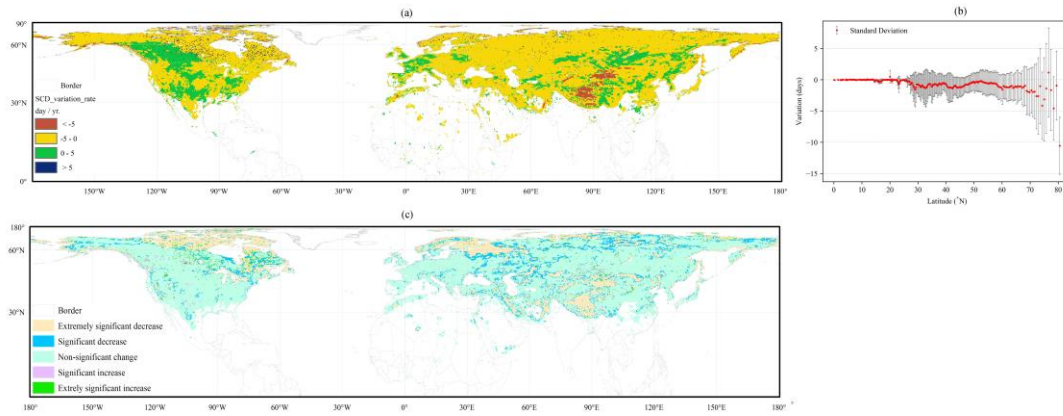
1
 2 Figure 9. The variation rate pattern of season average SD over the Northern Hemisphere for three snow
 3 cover season, fall (a, b; September to November), winter (c, d; December to February), spring (e, f;
 4 March to June) from 1992-2016. Black dots in (a, c, e) indicate that the changes are significant at 95%
 5 confidence level (CL). The zonal distribution in (b, d, f) are mapped at 0.25 degree resolution in
 6 latitude. The error bars in (b, d, f) is one times of standard deviation.

7



8

1 Figure 10. Interannual variation of [annual maximum snow mass \(A\)](#), [annual average snow mass \(B\)](#)
2 [and annual minimum snow mass \(C\)](#) over the Northern Hemisphere for three period 1992-2016 (black
3 line), 1992-2001 (blue line), and 2002-2016 (red line). Trends estimates were computed from least
4 squares. P is the confidence level for the coefficient estimates; R^2 is the goodness of fit coefficient.



5
6 Figure 11. The variation rate pattern of SCD (a) and their statistical significances (c) over the Northern
7 Hemisphere from 1992-2016. The zonal distribution in (b) are mapped at 0.25 degree resolution in
8 latitude. The error bars in (b) is one times of standard deviation.

9